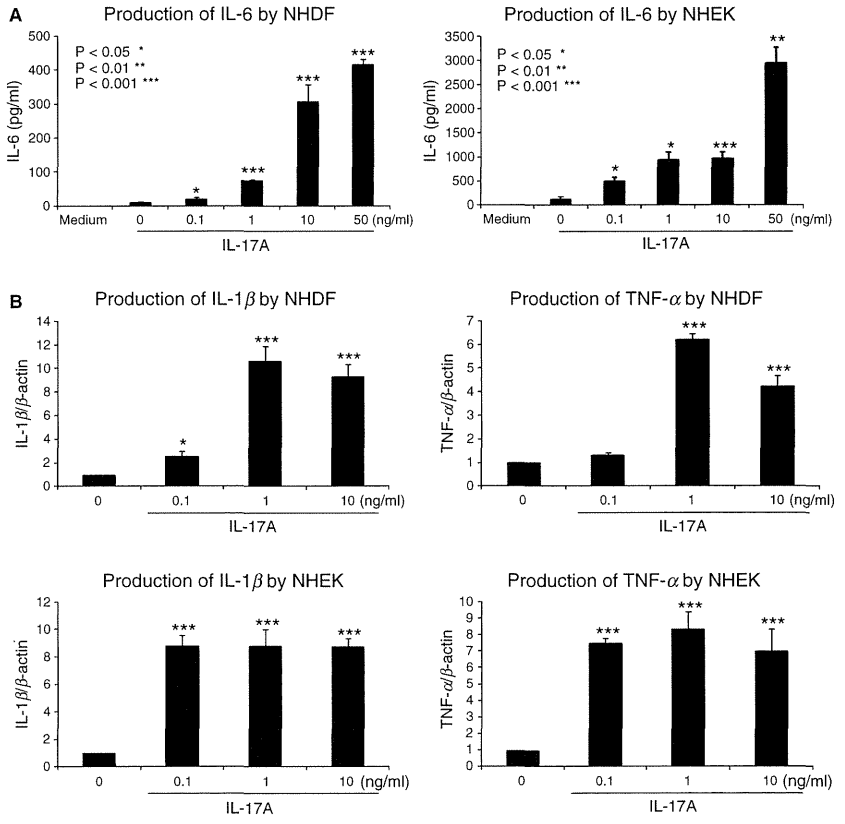

Figure 6. IL-17A induces the release of other Th17 cell-related cytokines from dermal fibroblasts and keratinocytes. (A) Human dermal fibroblasts and keratinocytes were incubated with recombinant IL-17A for 1 day at concentrations of 0.1, 1, 10, and 50 ng/ml in the culture medium, and the IL-6 secreted in the medium was measured by an ELISA. (B) After cells were incubated as in (A), the IL-1β and TNFα mRNA expression levels were measured by RT-PCR. β-actin was used as a housekeeping gene. *P < 0.05; **P < 0.01; ***P < 0.001 compared with the expression level of the untreated controls.

duction of these cytokines in a dose-dependent manner using both of these cell lines.

Cytokine-induced melanocyte dysfunction

Finally, we examined whether proinflammatory cytokines could directly induce melanocyte apoptosis and/or destruction in vitro. The cultured melanocytes were incubated with 1 and 10 ng/ml of recombinant IL-1β, IL-6, IL-17A, TNF-α, or all of the factors for 5 days, and then the melanocytes were observed microscopically under polarized light (Figure 7A). The cells were obviously aggregated and varied in shape after treatment with both the single cytokines and the cytokine cocktail, whereas the untreated cells and those treated with bFGF (basic fibroblast growth factor) grew with a spindle-shaped morphology. Staurosporine, a chemical that induces apoptosis by activating caspase-3, increased the number of round-shaped apoptotic melanocytes. TNF-α induced the greatest extent of melanocyte destruction compared with the other cytokines.

Next, melanocyte apoptosis was assessed by measuring caspase-3 activity after continuous treatment with 10 ng/ml of each of the individual cytokines and the cytokine cocktail. Staurosporine led to an increase in caspase-3 activity (Figure 7B), whereas there was no induction of caspase-3 activity following treatment with any of the cytokines. These results indicate that there appears to be direct inhibition of melanocyte activity by cytokines, rather than induction of cell apoptosis.

Discussion

In the present study, we identified a significant number of Th17 cells that had infiltrated vitiligo skin, and demonstrated the inhibitory effect of Th17 cell-related proinflammatory cytokines on melanocyte activity. We therefore hypothesize that the functional Th17 cell involvement in the initiation of psoriasis and atopic dermatitis may also play an important role in the pathogenesis of vitiligo. Although the precise pathogenic mechanisms underlying the induction of depigmentation in an immunological manner (Ongenae et al., 2003) still remain unknown, non-segmental vitiligo has been thought to be an autoimmune disease because of the high frequency of associated Hashimoto's thyroid disease (Daneshpazhooh et al., 2006; Hegedus et al., 1994; Schallreuter et al., 1994a), type I diabetes (Gould et al., 1985), collagen diseases with antinuclear antibodies (Mihailova et al., 1999), etc. Pathogenic antibodies were also detected in approximately 50% of vitiligo patients (Cui et al., 1992; Ruiz-Arguelles et al., 2007). With respect to the cellular immune condition, the infiltration of cytotoxic T cells targeting melanocyte-specific antigens in vitiligo lesions has been thought to play a critical role in hypopigmentation (Lang et al., 2001; Norris et al., 1994; Ogg et al., 1998). Recent reports have also suggested that there is the local environment of proinflammatory cytokines such as IL-1, IL-6, and TNF-α also contributes to the inhibition of melano-

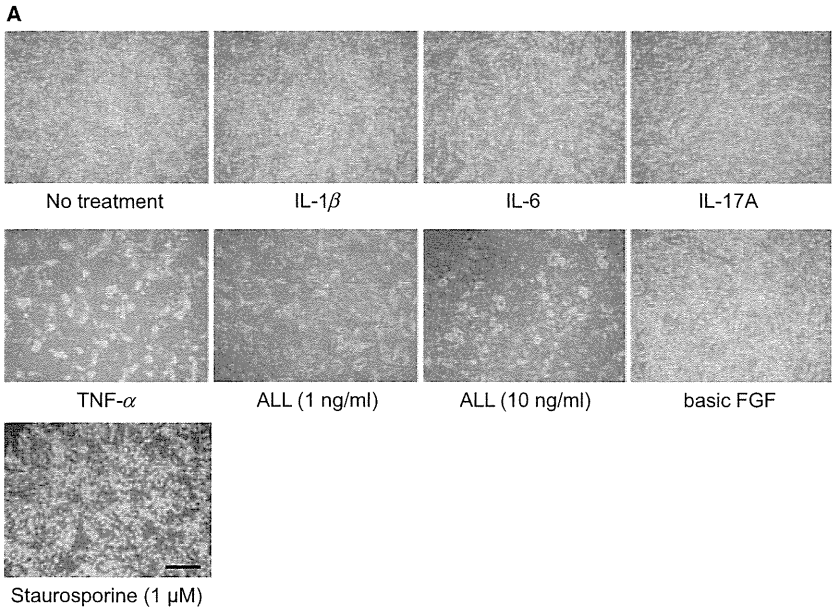

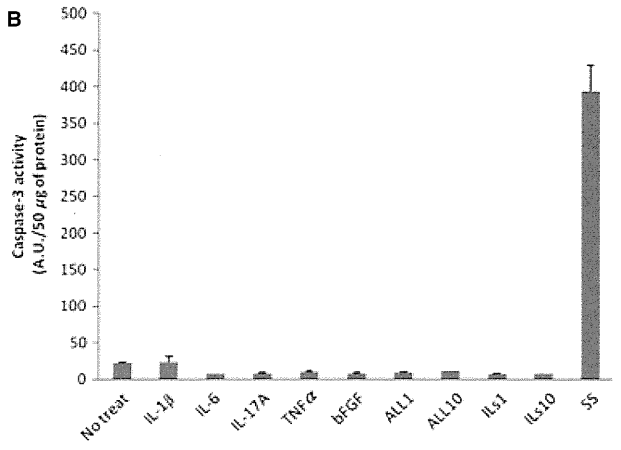

Figure 7. Proinflammatory cyotokines induce melanocyte cell destruction, but not apoptosis. (A) Human melanocytes were incubated with recombinant proinflammatory cytokines, including IL-1β, IL-6, IL-17A, and TNF-α continuously for 5 days at concentrations of 1 or 10 ng/ml in the culture medium. These cytokines were used either alone or in combination. Staurosporine was used as a positive control for cell apoptosis. The photographs were taken by a polarized microscope. The bar indicates 50 μm. (B) The absorbance at 450 nm was measured to determine the caspase-3 activity of the cells treated with cytokines. ILs indicates treatment together with IL-1β, IL-6 and IL-17A.

genesis and melanocyte survival (Moretti et al., 2002, 2009).

Direct regulation of melangenic factors by cytokines

The tyrosinase mRNA levels are generally correlated with tyrosinase activity (Ando et al., 1995). In our study, cytokine treatment decreased the mRNA levels of MITF, a transcription factor implicated in regulating melanogenic and antiapoptotic genes, and decreased the expression of genes encoding melanogenic enzymes such as tyrosinase, TYRP-1, and DCT (TYRP-2) in a dose-dependent manner. These results indicate that proinflammatory cytokines can play a pivotal role in the regulation of melanocyte fate through the downregulation of gene expression.

There have been several reports providing evidence that melanocyte functions are regulated by cytokines through several cellular signaling pathways (Kamaraju et al., 2002; Kholmanskikh et al., 2010). For example, IL-1β and 1α were found to direct the downregulation of MITF-M expression through the NF-κB and JNK pathways in two different melanoma cell lines (Kholmanskikh et al., 2010). IL-6/IL-6R signaling silenced the MITF promoter activity and this was mediated by Pax3 downregulation (Kamaraju et al., 2002). IL-6 is a pleiotropic cytokine involved in a variety of inflammatory responses. With regard to the relationship to Th17 cells, IL-6 is essential for induction of Th17 cell development and maintenance (Diveu et al., 2008). As the proinflammatory cytokines involved in Th17 cell fate include IL-1β and TGF-β in addition to IL-6, we examined the expression and activity of some of these cytokines in melanocytes.

Although there is no doubt that cellular and antibody-mediated immune reactions are related to melanocyte destruction, our data suggest that Th17 cells and skin-resident cells, particularly epidermal keratinocytes and dermal fibroblasts, might orchestrate a response that inhibits the stability of melanocytes in some vitiligo skin

through the production of proinflammatory cytokines. In addition, there might be an initial trigger attracting Th17 cells to vitiligo (or pre-vitiligo) skin.

A recent study using several skin samples showed greater numbers of Th17 cells, especially on the leading edge of vitiligo skin (Wang et al., 2011). In the present study, we confirm the presence of Th17 cell infiltration in vitiligo skin and suggest that there was a pathogenic function not only because of cytotoxic T cells but also because of Th17 cells and Th17 cell-related cytokines. Although we expected that there would be more infiltration of Th17 cells in the generalized type and progressive vitiligo compared with other clinical types, there was no significant correlation between the Th17 cell number and the clinical type and disease duration. It is possible that the small sample number, biopsy site, and preceding treatments, including the use of topical steroids, may have affected the status of inflammatory cell infiltration.

We observed that Th17 cells diffusely infiltrated the upper dermis, whereas $CD8^+$ cells were present beneath the basal membrane of the epidermis. In psoriatic skin, Th17 cells mainly infiltrate into the papillary dermis and epidermis. We therefore speculated that Th17 cells might be able to act on melanocytes by producing cytokines, rather than exerting a direct effect on the cells. To address this point, we stimulated dermal fibroblasts and keratinocytes using a characteristic pro-Th17 cytokine, IL-17A. IL-17A robustly upregulated the production of IL-1β and TNF-α by these skin-resident cells, suggesting the presence of mutual cytokine signaling between skin-resident cells and accumulating inflammatory cells. The melanocytes themselves can also synthesize IL-1α and β (Swope et al., 1994).

Previous studies have shown that cytokines associated with skin inflammation, such as IL-1β, IL-6, and TNF-α, inhibited melanin production in vitro (Englaro et al., 1999; Kamaraju et al., 2002; Kholmanskikh et al., 2010). We found that there were significant changes in the expression of epidermal cytokines in vitiligo lesions, where no melanocytes are present, compared with perilesional, non-lesional and healthy skin, where melanocytes are normally present. Therefore, it is conceivable that the cytokines derived from infiltrating cells, as well as the lesional epidermis, would be implicated in depigmented skin disorders. In the present study, treatment with a physiologically relevant concentration of IL-17A, in addition to IL-1β and IL-6, could directly regulate the expression of MITF and downstream molecules, and subsequently melanin synthesis, in human melanocytes.

Putative involvement of proinflammatory cytokines in vitiligo

Based on these experimental results, we propose the putative involvement of proinflammatory cytokines in the pathogenesis of vitiligo (Figure 8). Previous studies have shown that the perforin produced from CD8-positive cytotoxic T cells (Lang et al., 2001; Norris et al., 1994; Ogg et al., 1998), antimelanocyte antibodies (Baharav et al., 1996; Cui et al., 1992; Ruiz-Arguelles et al., 2007), and reactive oxygen species were related to the injury of melanocytes and were triggers for vitiligo (Schallreuter et al., 1994b). In the present study, we found a significant infiltration of Th17 cells in vitiligo skin, and demonstrated that Th17-related cytokines such as IL-1β, IL-6, and IL-17A directly or indirectly regulated melanin production and the expression of melanogenic and antiapoptotic molecules. The presence of a cytokine network and the secretion of IL-17A from Th17 cells may therefore represent a new mechanism underlying the pathogenesis of vitiligo concerning the downregulation of melanocyte activity. Indeed, the activation of the innate immune system may lead to the accumulation of Th17 cells in the vitiligo lesion as they do in psoriasis. In fact, the IL-1β released from lesional keratinocytes and melanocytes (Moretti et al., 2002, 2009; Swope et al., 1994) may act as the first inducer of the differentiation of naïve helper T cells into Th17 cells in vitiligo lesions. Thereafter, antimicrobial peptides derived from the lesional epidermis might induce the production of IL-17A by Th17 cells (Infante-Duarte et al., 2000).

Although psoriasis is one of representative skin disorders characterized by pathogenic Th17 cell infiltration, the phenotypic change in this disorder is not akin to that in vitiligo vulgaris. Because the final targets of IL-17A in

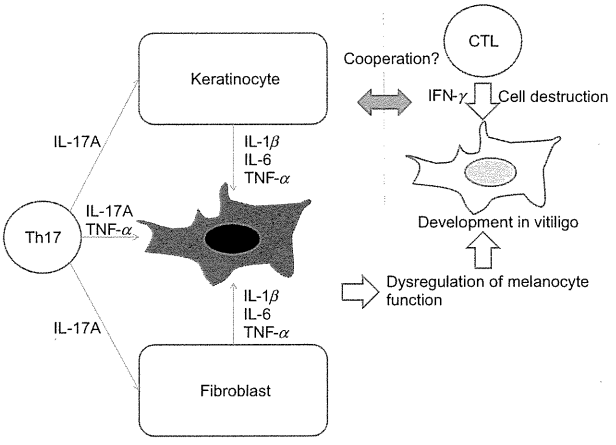

Figure 8. The proposed cues provided by Th17 cells and Th17 cell-related cytokines during the pathogenesis of autoimmune vitiligo. Previous known pathogenic mechanisms of melanocyte destruction in vitiligo include the presence of cytotoxic T cells attacking the melanocytes, local oxidative stress, and downregulation of melanogenesis-inducing factors in the vitiligo epidermis. The newly proposed phenomenon is that an imbalance in the local cytokine network is involved in the downregulation of melanocyte activity found in the present study. The IL-17A secreted from the Th17 cells in vitiligo skin can trigger the production of inhibitory cytokines from dermal fibroblasts and keratinocytes. IL-1β, IL-6, and TNF-α as well as IL17-A also repress melanocyte activity and induce melanocyte destruction.

vitiligo vulgaris and psoriasis are different, that is, melanocyte dysfunction in vitiligo vulgaris and abnormal keratinocyte turnover in psoriasis, Th17 cells may augment vitiliginous skin lesion formation in cooperation with skin-resident cells such as dermal fibroblasts and keratinocytes, as described previously. Microbial lipopeptides may then induce the cell polarization to Th17 cells, producing IL-17 and TNF-α as a result of the stimulation of the innate immune system in vitiligo (Infante-Duarte et al., 2000). Tip dendritic cell (tipCD)-like cells might also be involved in vitiligo formation, as previous reports demonstrated that the number of αDCs was increased in vitiligo vulgaris lesions or there was a unique distribution pattern of Langerhans cells present in such lesions (Mishima et al., 1972). Moreover, recent reports suggest that an altered innate immune response is observed in autoimmune vitiligo in concert with frequent *NALP1* gene mutations (Jin et al., 2007, 2010). An unrecognized micro-organism might stimulate the attending inflammatory cells through antimicrobial peptides and sequentially trigger vitiligo vulgaris. These issues should be clarified in further experiments.

Methods

Cell lines

HeMnMP, a moderately pigmented human melanocyte cell line, was obtained from Cascade Biologics and cultured in Medium 254 with human melanocyte growth supplement (Gibco Inc., Tokyo, Japan), and maintained at 37°C with 5% CO_2 in a humidified incubator. The cells were used for this study by the 5th passage to ensure melanin production. Dermal fibroblasts and epidermal keratinocytes were purchased from TAKARA BIO Inc., (Shiga, Japan) and maintained in DMEM containing 10% FCS and Medium 154 (Gibco Inc.), respectively.

Reagents

Human recombinant cytokines were purchased from Cell Signaling Technology (Tokyo, Japan) and synthetic melanin was from Sigma-Aldrich, Japan. The antibodies used for this study were as follows: anti-MITF mouse monoclonal Ab (D5) from Abcam (San Francisco, CA, USA), horseradish peroxidase (HRP)-conjugated anti-rabbit or mouse IgG from Cell Signaling Technology, anti-CD4 mouse monoclonal antibody from Novocastra Reagents (Tokyo, Japan), anti-CD8, -Foxp3, -CD20 and -Melan A mouse monoclonal antibodies from Dako (Tokyo, Japan), anti-IL17A goat monoclonal antibody from R&D (Minneapolis, MN, USA), Alexa Fluor 488-conjugated anti-mouse IgG and Alexa Fluor 555-conjugated anti-goat IgG from Invitrogen (Tokyo, Japan).

Tissue specimens

Approval for the use of human skin tissue samples was obtained from the local Ethical Committee of Osaka University Hospital and written informed consent was received from each patient after appropriate explanation of this study. Spindle-shaped skin biopsy specimens on the leading edge of vitiligo lesions were taken from 23 vitiligo patients. Twenty-three skin specimens were fixed in buffered 10% formalin and embedded in paraffin and processed for an immunohistochemical analysis as described below. Non-lesional skin from the matched vitiligo patients and normal skin from normal donors were processed as well.

RNA isolation and PCR assay for cytokine and melanocyte markers expression

Total RNA was extracted from HeMnMP cells using the TRIZOL reagent according to the manufacturer's instructions. Reverse transcription (RT) reactions were performed with Moloney murine leukemia virus reverse transcriptase (Promega, Tokyo, Japan) with oligo (dT) primers. For RT reaction of tissue RNA, total RNA was extracted from frozen vilitigo skin tissue using the Sepasol-RNA I reagent (NACALAI TESQUE, INC., Kyoto, Japan) according to the manufacturer's instructions. Genomic DNA contamination was removed by DNase I (TAKARA BIO INC.). The qRT assay was performed using an ABI prism 7900HT Sequence Detection System (Applied Biosystems, Carlsbad, CA, USA) according to the manufacturer's specifications. Briefly, the reaction mixture totaling 10 μl for each qRT consisted of 1 μl of cDNA generated from 250 ng of total RNA, 0.5 μM of Taqman probe labeled with FAM, the master mix for melanogenic markers and glyceraldehyde 3-phosphate dehydrogenase (GAPDH), or the Power SYBR green PCR master mix for cytokines. The mixture was processed by a two-step PCR method with an initial heating at 95°C for 10 min, followed by 40 cycles of denaturation at 95°C for 15 s, and annealing and extension at 60°C for 60 s for all genes. The obtained PCR amplification curves were analyzed using SDS software program, version 2.1 (Applied Biosystems). GAPDH was used as a control housekeeping gene, and the relative mRNA copy numbers were obtained as the ratio of the mRNA copies of each gene/copies of GAPDH. Each assay was performed at least three times. The specific probe and primers sequences used for this study were as follows:

MITF-M: 5′-AGCTCACAGCGTGTATTTTTCCCAC-3′
TYR: 5′-TCTCCTCTTGGCAGATTGTCTGTAG-3′
TRP-1: 5′-CTTTGTAACAGCACCGAGGATGGGC-3′
DCT: 5′-TGCAAGTGCACAGGAAACTTTGCCG-3′
BCL2: 5′-AACGGAGGCTGGGATGCCTTTGTGG-3′
GAPDH: 5′-GGGCGCCTGGTCACCAGGGCTGCTT-3′
IL-1β: Forward 5′- TGCACGCTCCGGGACTCACA-3′
IL-1 β: Reverse 5′- CGCCTTTGGTCCCTCCCAGG-3′
TNF-α: Forward 5′- CCCCTGACAAGCTGCCAGGC-3′
TNF-α: Reverse 5′- CAGCTCCACGCCATTGGCCA-3′

Reverse transcriptase PCR (RT-PCR) for IL-17A and cytokine receptor expression

To confirm IL-17A expression in vitiligo tissue and determine the expression levels of the cytokines and their receptors, we performed RT reactions with the above-mentioned procedure and PCR with an initial heating at 95°C for 10 min, followed by 40 cycles of denaturation at 95°C for 15 s, and annealing and extension at appropriate temperatures for 60 s for all genes. Samples were then processed for electrophoresis. The following primer sets were used:

IL-17A: Forward 5′- ACAAACTCATCCATCCCCAG-3′
IL-17A: Reverse 5′- GTGAGGTGGATCGGTTGTAG-3′
IL-1R1: Forward 5′-CCCGTTGCAGGAGACGGAGG-3′
IL-1R1: Reverse 5′-CCACCCAGCCAGCTGAAGCC-3′
IL-1R2: Forward 5′-CTTTAAAGCTGCTTCTGCCACGTG-3′
IL-1R2: Reverse 5′-CATTGCCCGTCCACCACAGCA-3′
IL-6R: Forward 5′-GAGTTCGGGCAAGGCGAGTGG-3′
IL-6R: Reverse 5′-AGGCTCCCTCCAGCAACCAGGAA-3′
IL-17RA: Forward 5′-AAGCCTCAGAACGTTCGTTCGCT-3′
IL-17RA: Reverse 5′-TTGGGCAGGTGGTGAACGGT-3′

Melanin content assay

Melanin production was determined as described previously (Virador et al., 1999). Briefly, 2 days after the plating of 1×10^5 melanocytes into a 6-well culture dish, we performed 5 days of

sequential treatment with 1–10 ng/ml of recombinant cytokines. To determine the melanin content, the pellets of treated cells were dissolved in 200 μl of 1 N NaOH for 30 min, and the concentrations of melanin were calculated by measuring the absorbance at 450 nm. Synthetic melanin was used to generate a standard curve. The melanin content was expressed as nanograms of melanin per microgram of total protein, and the ratio was compared among the samples.

Immunostaining

Vitiliginous skin specimens were processed after receiving written informed consent from vitiligo patients (n = 23). Paraffin-embedded archival tissues were deparaffinized with absolute xylene and dehydrated in a sequential ethanol dilution series. The deparaffinized sections were boiled in an oil bath for 15 min in 10 mM Tris-1 mM EDTA buffer (pH 9.0) for antigen retrieval. The slides were blocked by the Protein Block Serum-Free solution (Dako) for 15 min and incubated with an anti-IL-17A goat monoclonal Ab (×200) at 4°C overnight. After being washed with TBS (pH 7.6), the slides were incubated with Alexa Fluor 555-conjugated anti-goat IgG Ab (×200) and then incubated with anti-CD4 mouse monoclonal Ab (×25) at RT for 1 h, followed by incubation with Alexa Fluor 488-conjugated anti-mouse IgG Ab (×200). The following primary antibodies were used to assess the expression of melanocyte markers and the melanosomal protein MART1: anti-CD8 mouse monoclonal Ab (×25), anti-CD20 mouse monoclonal Ab (×25), anti-Foxp3 mouse monoclonal Ab (×50), and anti-Melan A (recognizing the MART-1 antigen) mouse monoclonal Ab (×50). These antibodies were provided by DAKO Inc.

For the immunocytochemistry analyses, the HeMnMP cells cultured in two-well Lab-Tek chamber slides (Nunc, Tokyo, Japan) were incubated with an anti-MITF mouse monoclonal antibody (×25) at 4°C overnight, followed by incubation with Alexa Fluor 555-conjugated anti-mouse IgG (×500) as the secondary antibody. The mouse isotype IgG was used as a negative control for staining. Nuclei were counterstained after DAPI staining (×1000).

Quantitative analysis of proinflammatory cytokines after the treatment with Th17-related cytokines

To assess the cell–cell interactions between the cells in the skin occurring as a result of paracrine cytokine production, the concentrations of proinflammatory cytokines such as IL-6 and IL-1β in the culture supernatant from dermal fibroblasts was measured 24 h after treatment with recombinant IL-17A using an ELISA kit from R&D.

Apoptosis assay

We determined the cleaved caspase-3 activity following treatment with recombinant cytokines using an apoptosis detection kit (R&D Systems). Briefly, cultured melanocytes were treated with cytokines (1 or 10 ng/ml) for 5 days. The culture medium was not changed until cell extraction, and cytokines were added in the culture medium every day. Thereafter, in addition to observation of melanocyte morphology under a polarized microscope, the melanocytes were processed for measurement of cleaved caspase-3 activity according to manufacturer's instructions.

Statistical analysis

The unpaired *t*-test was used for the analysis of differences in gene and protein expression. The results are shown as the means + SD. A value of $P < 0.05$ (two-tailed) was considered significant. All statistical analyses were performed using the PRISM software program, version 5 (GraphPad Software Inc., La Jolla, CA, USA).

Acknowledgements

We thank Kenju Nishida, Eriko Nobuyoshi, and Tomoka Matsumura for their expert technical assistance. This work was supported in part by a grant from the Ministry of Education, Culture, Sports, Science and Technology of Japan and a grant from the Ministry of Health, Labor and Welfare.

References

Ando, H., Itoh, A., Mishima, Y., and Ichihashi, M. (1995). Correlation between the number of melanosomes, tyrosinase mRNA levels, and tyrosinase activity in cultured murine melanoma cells in response to various melanogenesis regulatory agents. J. Cell. Physiol. *163*, 608–614.

Asarch, A., Barak, O., Loo, D.S., and Gottlieb, A.B. (2008). Th17 cells: a new therapeutic target in inflammatory dermatoses. J. Dermatolog. Treat. *19*, 318–326.

Baharav, E., Merimski, O., Shoenfeld, Y., Zigelman, R., Gilbrud, B., Yecheskel, G., Youinou, P., and Fishman, P. (1996). Tyrosinase as an autoantigen in patients with vitiligo. Clin. Exp. Immunol. *105*, 84–88.

Basak, P.Y., Adiloglu, A.K., Ceyhan, A.M., Tas, T., and Akkaya, V.B. (2009). The role of helper and regulatory T cells in the pathogenesis of vitiligo. J. Am. Acad. Dermatol. *60*, 256–260.

Bassiouny, D.A., and Shaker, O. (2011). Role of interleukin-17 in the pathogenesis of vitiligo. Clin. Exp. Dermatol. *36*, 292–297.

Caixia, T., Hongwen, F., and Xiran, L. (1999). Levels of soluble interleukin-2 receptor in the sera and skin tissue fluids of patients with vitiligo. J. Dermatol. Sci. *21*, 59–62.

Chalraborty, A., and Pawelek, J. (1993). MSH receptors in immortalized human epidermal keratinocytes: a potential mechanism for coordinate regulation of the epidermal-melanin unit. J. Cell. Physiol. *157*, 344–350.

Cui, J., Harning, R., Henn, M., and Bystryn, J.C. (1992). Identification of pigment cell antigens defined by vitiligo antibodies. J. Invest. Dermatol. *98*, 162–165.

Daneshpazhooh, M., Mostofizadeh, G.M., Behjati, J., Akhyani, M., and Robati, R.M. (2006). Anti-thyroid peroxidase antibody and vitiligo: a controlled study. BMC Dermatol. *6*, 3.

Diveu, C., Mcgeachy, M.J., and Cua, D.J. (2008). Cytokines that regulate autoimmunity. Curr. Opin. Immunol. *20*, 663–668.

Englaro, W., Bahadoran, P., Bertolotto, C., Busca, R., Derijard, B., Livolsi, A., Peyron, J.F., Ortonne, J.P., and Ballotti, R. (1999). Tumor necrosis factor alpha-mediated inhibition of melanogenesis is dependent on nuclear factor kappa B activation. Oncogene *18*, 1553–1559.

Fitch, E.L., Rizzo, H.L., Kurtz, S.E., Wegmann, K.W., Gao, W., Benson, J.M., Hinrichs, D.J., and Blauvelt, A. (2009). Inflammatory skin disease in K5.hTGF-beta1 transgenic mice is not dependent on the IL-23/Th17 inflammatory pathway. J. Invest. Dermatol. *129*, 2443–2450.

Gould, I.M., Gray, R.S., Urbaniak, S.J., Elton, R.A., and Duncan, L.J. (1985). Vitiligo in diabetes mellitus. Br. J. Dermatol. *113*, 153–155.

Hegedus, L., Heidenheim, M., Gervil, M., Hjalgrim, H., and Hoier-Madsen, M. (1994). High frequency of thyroid dysfunction in patients with vitiligo. Acta Derm. Venereol. *74*, 120–123.

Howitz, J., Brodthagen, H., Schwartz, M., and Thomsen, K. (1977). Prevalence of vitiligo. Epidemiological survey on the Isle of Bornholm, Denmark. Arch. Dermatol. *113*, 47–52.

Infante-Duarte, C., Horton, H.F., Byrne, M.C., and Kamradt, T. (2000). Microbial lipopeptides induce the production of IL-17 in Th cells. J. Immunol. *165*, 6107–6115.

Jin, Y., Mailloux, C.M., Gowan, K., Riccardi, S.L., Laberge, G., Bennett, D.C., Fain, P.R., and Spritz, R.A. (2007). NALP1 in vitiligo-associated multiple autoimmune disease. N. Engl. J. Med. *356*, 1216–1225.

Jin, Y., Riccardi, S.L., Gowan, K., Fain, P.R., and Spritz, R.A. (2010). Fine-mapping of vitiligo susceptibility loci on chromosomes 7 and 9 and interactions with NLRP1 (NALP1). J. Invest. Dermatol. *130*, 774–783.

Kamaraju, A.K., Bertolotto, C., Chebath, J., and Revel, M. (2002). Pax3 down-regulation and shut-off of melanogenesis in melanoma B16/F10.9 by interleukin-6 receptor signaling. J. Biol. Chem. *277*, 15132–15141.

Kholmanskikh, O., Van Baren, N., Brasseur, F., Ottaviani, S., Vanacker, J., Arts, N., Van Der Bruggen, P., Coulie, P., and De Plaen, E. (2010). Interleukins 1alpha and 1beta secreted by some melanoma cell lines strongly reduce expression of MITF-M and melanocyte differentiation antigens. Int. J. Cancer *127*, 1625–1636.

Kingo, K., Aunin, E., Karelson, M., Ratsep, R., Silm, H., Vasar, E., and Koks, S. (2008). Expressional changes in the intracellular melanogenesis pathways and their possible role in the pathogenesis of vitiligo. J. Dermatol. Sci. *52*, 39–46.

Kolls, J.K., and Linden, A. (2004). Interleukin-17 family members and inflammation. Immunity *21*, 467–476.

Lang, K.S., Caroli, C.C., Muhm, A., Wernet, D., Moris, A., Schittek, B., Knauss-Scherwitz, E., Stevanovic, S., Rammensee, H.G., and Garbe, C. (2001). HLA-A2 restricted, melanocyte-specific CD8(+) T lymphocytes detected in vitiligo patients are related to disease activity and are predominantly directed against MelanA/MART1. J. Invest. Dermatol. *116*, 891–897.

Levy, C., Khaled, M., and Fisher, D.E. (2006). MITF: master regulator of melanocyte development and melanoma oncogene. Trends Mol. Med. *12*, 406–414.

Liang, S.C., Tan, X.Y., Luxenberg, D.P., Karim, R., Dunussi-Joannopoulos, K., Collins, M., and Fouser, L.A. (2006). Interleukin (IL)-22 and IL-17 are coexpressed by Th17 cells and cooperatively enhance expression of antimicrobial peptides. J. Exp. Med. *203*, 2271–2279.

Mihailova, D., Grigorova, R., Vassileva, B., Mladenova, G., Ivanova, N., Stephanov, S., Lissitchky, K., and Dimova, E. (1999). Autoimmune thyroid disorders in juvenile chronic arthritis and systemic lupus erythematosus. Adv. Exp. Med. Biol. *455*, 55–60.

Mishima, Y., Kawasaki, H., and Pinkus, H. (1972). Dendritic cell dynamics in progressive depigmentations. Distinctive cytokinetics of -dendritic cells revealed by electron microscopy. Arch. Dermatol. Forsch. *243*, 67–87.

Moretti, S., Spallanzani, A., Amato, L., Hautmann, G., Gallerani, I., Fabiani, M., and Fabbri, P. (2002). New insights into the pathogenesis of vitiligo: imbalance of epidermal cytokines at sites of lesions. Pigment Cell Res. *15*, 87–92.

Moretti, S., Fabbri, P., Baroni, G., Berti, S., Bani, D., Berti, E., Nassini, R., Lotti, T., and Massi, D. (2009). Keratinocyte dysfunction in vitiligo epidermis: cytokine microenvironment and correlation to keratinocyte apoptosis. Histol. Histopathol. *24*, 849–857.

Norris, D.A., Horikawa, T., and Morelli, J.G. (1994). Melanocyte destruction and repopulation in vitiligo. Pigment Cell Res. *7*, 193–203.

Ogg, G.S., Rod Dunbar, P., Romero, P., Chen, J.L., and Cerundolo, V. (1998). High frequency of skin-homing melanocyte-specific cytotoxic T lymphocytes in autoimmune vitiligo. J. Exp. Med. *188*, 1203–1208.

Okamoto, T., Irie, R.F., Fujii, S., Huang, S.K., Nizze, A.J., Morton, D.L., and Hoon, D.S. (1998). Anti-tyrosinase-related protein-2 immune response in vitiligo patients and melanoma patients receiving active-specific immunotherapy. J. Invest. Dermatol. *111*, 1034–1039.

Ongenae, K., Van Geel, N., and Naeyaert, J.M. (2003). Evidence for an autoimmune pathogenesis of vitiligo. Pigment Cell Res. *16*, 90–100.

Ratsep, R., Kingo, K., Karelson, M., Reimann, E., Raud, K., Silm, H., Vasar, E., and Koks, S. (2008). Gene expression study of IL10 family genes in vitiligo skin biopsies, peripheral blood mononuclear cells and sera. Br. J. Dermatol. *159*, 1275–1281.

Ruiz-Arguelles, A., Brito, G.J., Reyes-Izquierdo, P., Perez-Romano, B., and Sanchez-Sosa, S. (2007). Apoptosis of melanocytes in vitiligo results from antibody penetration. J. Autoimmun. *29*, 281–286.

Schallreuter, K.U., Lemke, R., Brandt, O., Schwartz, R., Westhofen, M., Montz, R., and Berger, J. (1994a). Vitiligo and other diseases: coexistence or true association? Hamburg study on 321 patients. Dermatology *188*, 269–275.

Schallreuter, K.U., Wood, J.M., Pittelkow, M.R., Gutlich, M., Lemke, K.R., Rodl, W., Swanson, N.N., Hitzemann, K., and Ziegler, I. (1994b). Regulation of melanin biosynthesis in the human epidermis by tetrahydrobiopterin. Science *263*, 1444–1446.

Swope, V.B., Sauder, D.N., Mckenzie, R.C., Sramkoski, R.M., Krug, K.A., Babcock, G.F., Nordlund, J.J., and Abdel-Malek, Z.A. (1994). Synthesis of interleukin-1 alpha and beta by normal human melanocytes. J. Invest. Dermatol. *102*, 749–753.

Virador, V.M., Kobayashi, N., Matsunaga, J., and Hearing, V.J. (1999). A standardized protocol for assessing regulators of pigmentation. Anal. Biochem. *270*, 207–219.

Wang, C.Q., Cruz-Inigo, A.E., Fuentes-Duculan, J., Moussai, D., Gulati, N., Sullivan-Whalen, M., Gilleaudeau, P., Cohen, J.A., and Krueger, J.G. (2011). Th17 cells and activated dendritic cells are increased in vitiligo lesions. PLoS ONE *6*, e18907.

Wilson, N.J., Boniface, K., Chan, J.R. et al. (2007). Development, cytokine profile and function of human interleukin 17-producing helper T cells. Nat. Immunol. *8*, 950–957.

Supporting information

Additional Supporting Information may be found in the online version of this article:

Figure S1. Coculture of helper T cells and melanocytes, and measurement of the expression of melanogenic markers.

Please note: Wiley-Blackwell are not responsible for the content or functionality of any supporting materials supplied by the authors. Any queries (other than missing material) should be directed to the corresponding author for the article.

EXD Journal Name | 1454 Manuscript No. | B | Dispatch: 3.2.12 | Journal: EXD | CE: Deepika K | Author Received: | No. of pages: 6 | PE: Sathya Kala

DOI:10.1111/j.1600-0625.2012.01454.x
www.blackwellpublishing.com/EXD

Original Article

Periostin, a matricellular protein, accelerates cutaneous wound repair by activating dermal fibroblasts

Kanako Ontsuka[1*], Yorihisa Kotobuki[2,3*], Hiroshi Shiraishi[1], Satoshi Serada[3], Shoichiro Ohta[4], Atsushi Tanemura[2], Lingli Yang[2,3], Minoru Fujimoto[3], Kazuhiko Arima[1], Shoichi Suzuki[1], Hiroyuki Murota[2], Shuji Toda[5], Akira Kudo[6], Simon J. Conway[7], Yutaka Narisawa[8], Ichiro Katayama[2], Kenji Izuhara[1] and Tetsuji Naka[3]

[1]Division of Medical Biochemistry, Department of Biomolecular Sciences, Saga Medical School, Saga, Japan; [2]Department of Dermatology, Osaka University Graduate School of Medicine, Suita, Japan; [3]Laboratory for Immune Signal, National Institute of Biochemical Innovation, Ibaraki, Japan; [4]Department of Laboratory Medicine, Saga Medical School, Saga, Japan; [5]Department of Pathology and Biodefense, Saga Medical School, Saga, Japan; [6]Department of Biological Information, Tokyo Institute of Technology, Yokohama, Japan; [7]Program in Developmental Biology and Neonatal Medicine, Herman B. Wells Center for Pediatric Research, Indiana University School of Medicine, Indianapolis, IN, USA; [8]Department of Dermatology, Saga Medical School, Saga, Japan

Correspondence: Kenji Izuhara, Division of Medical Biochemistry, Department of Biomolecular Sciences, Saga Medical School, 5-1-1, Nabeshima, Saga 849-8501, Japan, Tel.: +81-952-34-2261, Fax: +81-952-34-2058, e-mail: kizuhara@cc.saga-u.ac.jp

**These two authors contributed equally to this work.*

Abstract: Cutaneous wound repair is a highly ordered and well-coordinated process involving various cell lineages and many molecular effectors. Cell–matrix interactions through integrin molecules provide key signals important for wound repair. Periostin is a matricellular protein that may provide signals important during tissue development and remodelling by interacting with several integrin molecules, via the phosphatidylinositol 3-kinase/Akt and MAP kinase pathways. In this study, we examined the role of periostin in the process of cutaneous wound repair using periostin-deficient mice and by analysing the effects of periostin on dermal fibroblasts. We first determined the expression profile and localization of periostin in a well-characterized wound repair model mice. Periostin was robustly deposited in the granulation tissues beneath the extended epidermal wound edges and at the dermal–epidermal junctions in wounded mice. Moreover, periostin-deficient mice exhibited delayed *in vivo* wound repair, which could be improved by direct administration of exogenous periostin. *In vitro* analyses revealed that loss of periostin impaired proliferation and migration of dermal fibroblasts, but exogenous supplementation or enforced periostin expression enhanced their proliferation. Combined, these results demonstrate that periostin accelerates the process of cutaneous wound repair by activating fibroblasts.

Key words: fibroblast – matrix – mice – periostinintegrin – wound repair

Accepted for publication 18 January 2012

Introduction

Cutaneous wound repair is a physiological function that is well ordered and highly coordinated (1–4). The process of repair is divided into three phases: inflammation, new tissue formation and remodelling. In the inflammatory phase beginning with haemostasis, first neutrophils and later macrophages are recruited to the wound site. These infiltrated macrophages not only exert their phagocytic activities but also accelerate re-epithelialization and granulation tissue formation. During new tissue formation, the process of re-epithelialization occurs via extension of wedge-shaped keratinocyte lineage. Fibroblasts and macrophages subsequently form the granulation tissues, assisting in the key process of re-epithelialization. Finally, during the remodelling phase, most of the endothelial cells, macrophages and myofibroblasts undergo apoptosis, leaving a scar containing a few cells with an extensive extracellular matrix (ECM) deposition dominated by collagens.

In the new tissue forming phase, fibroblasts produce mainly collagens and other ECM components such as glycosaminoglycans and proteoglycans, contributing to the formation of granulation tissues, with the provisional fibrin-based matrix eventually being replaced (1,5–7). In addition, fibroblasts secrete various growth factors – fibroblast growth factor-2 (FGF-2)/basic FGF, FGF-7/keratinocyte growth factor, FGF-10, epidermal growth factor and transforming growth factor-β (TGF-β) – which can all affect the process of keratinocyte re-epithelialization (8). TGF-β1 can also drive differentiation of some fibroblasts into transformed myofibroblasts that express α-smooth muscle actin (α-SMA) (9), which are able to contract to draw the wound edges together (1–4). This combination of growth factor receptor–mediated signals and integrin-mediated signals are thought to result in growth, migration, survival, spreading and ECM production responses within the wound fibroblasts (10–12). However, the underlying mechanism of fibroblast activation during cutaneous wound repair has not yet been fully understood.

Periostin is an ECM protein belonging to the fasciclin family (13,14) and is a newly characterized matricellular protein whose main functions are thought to be modulation of cell–matrix interactions and cell functions rather than playing a direct structural role (15,16). Periostin is known to interact with several integrin molecules, specifically $\alpha_v\beta_3$ or $\alpha_v\beta_5$ on cell surfaces, activating the phosphatidylinositol 3-kinase (PI3K)/Akt and MAP kinase pathways during tissue development and remodelling (13,14). We and others have demonstrated the presence of periostin in fibrotic areas in various pathological conditions: bronchial

asthma (17–19), pulmonary fibrosis (20), myocardial infarction (21), valvular heart disease (22), cystic fibrosis (23) and proliferative diabetic retinopathy (24). Further, it has been shown that the biological functions of periostin as a matricellular protein rather than structural player are important for the pathogenesis of some of these diseases. For instance, periostin affects eosinophils and/or epithelial cells in bronchial asthma, enhancing eosinophil migration and/or activating TGF-β, respectively (25,26). Moreover, in the healing process of myocardial infarction, periostin may enhance cardiac repair via stimulation of myocyte proliferation (27), although whether this is a direct mechanism or via adjacent cardiac fibroblasts remains controversial (28). Furthermore, periostin accelerates the development of various tumors by promoting cancer cell survival, epithelial–mesenchymal transition, invasion and metastasis (29,30). In contrast, the physiological roles of periostin remain poorly understood, except for several studies using periostin-deficient mice that suggest non-replaceable roles for periostin during development of bone, tooth and heart valves (14,31).

Importantly for this study, periostin is known to be highly expressed in wounds, suggesting its involvement in the process of wound repair (32,33). To directly examine the role of periostin within the process of cutaneous wound repair, we employed both *in vivo* and *in vitro* approaches using systemic periostin-deficient mice, exogenous periostin supplementation and a well-characterized mouse wound repair model. Significantly, wound repair is delayed in periostin-deficient mice. Furthermore, exogenous periostin up-regulates proliferation and migration of the dermal fibroblasts, which suggests this may be the mechanism how periostin accelerates cutaneous wound repair. These results demonstrate that periostin is required for the process of cutaneous wound repair, highlighting its physiological role, and suggest that periostin may be a useful candidate to therapeutically speedup wound repair.

Methods

Mice

Eight- to twelve-week-old C57BL/6 or BALB/c mice (Japan SLC, Japan), periostin-deficient (*Postn*$^{-/-}$, C57BL/6 or BALB/c background) mice, were used (14,21). Experiments were undertaken following the guidelines for care and use of experimental animals required by the Japanese Association for Laboratory Animals Science (1987).

Mouse wound repair model

Mice were anaesthetized by inhalation of halothane or intraperitoneal injection of pentobarbital. After their backs were shaved, 8- or 10-mm diameter full-thickness wounds were generated using disposable biopsy punches (Kai Industries, Seki, Japan). Wound sizes were measured longitudinally with a slide calliper. Wound tissues were excised at indicated time points postinjury and used for quantitative RT-PCR, Western blotting or histological analysis. Following fixation in 3.7% formaldehyde and embedding in paraffin, histological analysis was performed on serial sections from spanning the central portion of the wound and stained with haematoxylin and eosin (H&E), Masson's trichrome and/or via immunohistochemical staining as previously described (18,20). In selected experiments, 2 μg recombinant mouse periostin (R&D Systems, Minneapolis, MN, USA) was painted onto the wound lesions every 2 days from day 1 to 9.

Quantitative RT-PCR

Quantitative RT-PCR was used to measure periostin as previously described (18). Briefly, RNA from wound site was isolated using an RNeasy Mini kit (Qiagen Japan, Tokyo, Japan), and the RT reaction was performed using a QuantiTect Reverse Transcription Kit (Qiagen Japan). Quantitative analysis was achieved using Applied Biosystems StepOnePlus™ Real-Time PCR System (Life Technologies Japan, Tokyo, Japan). The primer sequence and PCR conditions are referred to the Data S1.

Confocal microscopy

Excised wound tissues were fixed with 3.7% formaldehyde and embedded in paraffin. After blocking with 2% BSA, the wax sections were stained using polyclonal anti-periostin Ab, previously prepared (18) followed by Alexa488-labelled anti-rabbit IgG Ab (Invitrogen, Carlsbad, CA, USA). The sections were mounted by Dako fluorescent mounting medium (Dako, Glostrup, Denmark) and then examined by LSM5 PASCAL G/B microscope (Carl Zeiss Japan, Tokyo, Japan).

Transduction of periostin into MEFs

Mouse full-length *Postn* cDNA was cloned (ENSMUST000000-81564) from MEF. Overexpression of mouse periostin into wild-type or periostin-deficient MEFs was performed using retroviral transduction of pMXs-puro vector [provided by Dr. Toshio Kitamura, Tokyo University, Tokyo, Japan (34)]. As a control, an empty vector was used alongside periostin-containing vector. After transduction, only infected cells were selected by 1 μg/ml puromycin (InvivoGen, San Diego, CA, USA).

Proliferation assay

Proliferation of fibroblasts was examined using the Cell Counting Reagent SF (Nacalai Tesque, Kyoto, Japan) according to the manufacturer's recommendations. In selected experiments, after 4-h serum starvation, dermal fibroblasts were seeded on the specified concentration of recombinant periostin (as described previously).

Statistical analyses

The results are presented as means + SD. Analysis was carried out using the two-sided, unpaired Student's *t*-test or the two-sided Welch test. Multiple comparisons between groups were performed by Fisher's or Dunnett's methods. We considered values to be significant when $P < 0.05$.

Results

Periostin expression is induced in wound tissues

We first analysed the expression of periostin in wound tissues. In C57BL/6 mice, periostin mRNA started to increase at day 1 after injury and peaked at day 7, decreasing thereafter (Fig. 1a, $n = 8$). Correspondingly, periostin protein levels peaked at day 7–10 and were sustained until day 18 (Fig. 1b). Wounded mice on the BALB/c background showed almost identical kinetics of periostin temporal changes at both the mRNA and protein levels (Fig. S1, $n = 8$). We then examined whether the localization of periostin was altered in wounded tissues. In the normal unwounded skin, periostin was expressed weakly at the dermal–epidermal junction and relatively robustly around the hair follicles (Figs 1c and S2). At day 6, when the wound was still open with hypertrophic epidermal wound edges and granulation tissues formed beneath these edges, periostin was now strongly expressed in the dermal–epidermal junction at these edges and within the granulation tissues. At day 9, when the wound was closed, significant expression of periostin was still observed in the granulation tissues beneath

COLOR

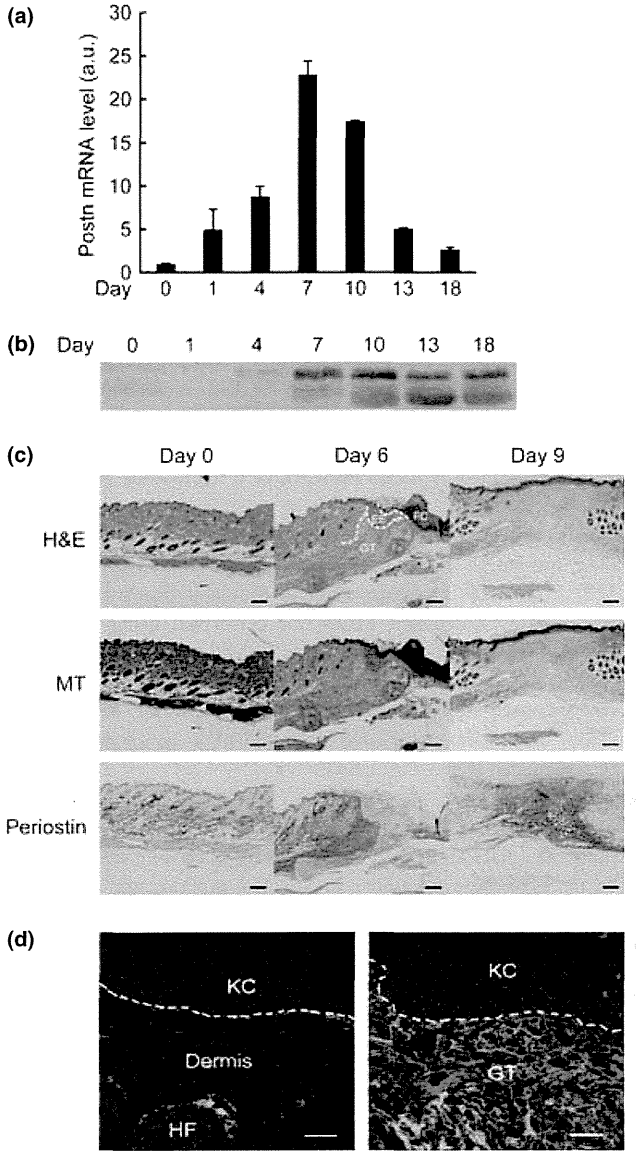

Figure 1. Periostin expression in wounded tissues. (a, b) Analysis of expression of periostin mRNA (a) or periostin protein (b) in wounded skin of C57BL/6 (n = 8) mice following the indicated amount of days postinjury. In b, experiments were repeated three times, and the representative combined data are depicted. (c) Wound sites stained with H&E, Masson trichrome (MT) and anti-periostin Ab from wild-type C57BL/6 mice for the indicated amount of days postinjury. FC, fibrin clot; EE, epidermal edge; GT, granulation tissue. Scale bar represents 200 μm. (d) Confocal microscopic imaging of wounds at day 6 is shown. Left and right panels depict non-wounded or wounded areas, respectively. Green and red represent periostin and the intrinsic fluorescence of cells, respectively. Scale bar represents 20 μm. KC, keratinocyte; GT, granulation tissue; HC, hair follicle.

the re-epithelialized wounds. To assess localization, we double-stained periostin (appears green), and this enabled us to conclude that periostin was deposited only at the border between the epidermis and the dermis and around hair follicles in the non-wounded sites, whereas periostin was deposited in the interspace regions of the red-staining granulation tissues in the wounded sites (Fig. 1d). These results demonstrate that periostin is induced during wound repair, suggesting that periostin may play a role in the repair process as well as being a useful marker of well-organized wound repair.

Periostin is required for efficient wound repair in mice

To test the functional requirement of periostin in wound repair, we used periostin-deficient ($Postn^{-/-}$) mice to perform wounding and assess their response. The wound sizes during the healing time course were significantly reduced in $Postn^{+/+}$ mice in C57BL/6 background (Fig. 2a,b, n = 10 for each genotype, $P < 0.05$ at day 3, 5 and 11, $P < 0.01$ at day 7) and in $Postn^{+/-}$ mice in a BALB/c background (Fig. S3, n = 3 for $Postn^{-/-}$ and n = 6 for $Postn^{+/-}$, $P < 0.05$ at day 3 and 10, $P < 0.001$ at day 13) than those observed in age-matched litter $Postn^{-/-}$ mice. Accordingly, the time intervals to completely close the wounds were significantly extended in $Postn^{-/-}$ mice than within $Postn^{+/+}$ mice (Fig. S4, 14.1 ± 0.74 days vs 15.9 ± 1.6 days, $P < 0.05$).

When we painted recombinant periostin protein onto the wounded area of $Postn^{-/-}$ mice every 2 days, starting day 1 after injury to day 9, the observed slower wound repair was subsequently accelerated (Fig. 2c,d upper panel, n = 10 for each group, the wound sizes: $P < 0.01$ at day 3, $P < 0.001$ at day 5 and 7, the time interval required to close the wounds: 15.9 ± 1.6 days vs 13.8 ± 1.4 days, $P < 0.01$). Moreover, the effects of administering exogenous periostin on accelerating wound repair were observed even in $Postn^{+/+}$ mice (Fig. 2c lower panel and Fig. S4, the wound sizes: $P < 0.05$ at day 7, the time interval to close the wounds: 14.1 ± 0.74 days vs 12.8 ± 1.1 days, $P < 0.01$). Thus, these results clearly demonstrate the requirement and positive effect of periostin within the wound repair process in mice.

Effect of periostin on proliferation in dermal fibroblasts

It has been shown that periostin can bind $\alpha_v\beta_3$ and $\alpha_v\beta_5$ integrin heterodimers (13,14) and that signalling via integrin molecules is imperative for cell proliferation and migration (10–12). Thus, we confirmed that α_v, β_3 and β_5 integrins, but not β_4 integrin, were expressed in human dermal fibroblasts, although A431 cells express β_4 integrin (Fig. S5A). Furthermore, when we stimulated human dermal fibroblasts with recombinant periostin, phosphorylation of downstream molecules of integrins focal adhesion kinase [FAK, STAT3, Akt and p44/42MAPK] was also observed (Fig. S5B). These results suggest that the interaction of periostin with human dermal fibroblasts is able to activate key signalling pathways via integrins present in the wound.

The present observation that periostin was strongly deposited within the granulation tissues beneath the hypertrophic epidermal wound edges raised the possibility that periostin may directly affect fibroblast proliferation, thereby accelerating the repair process. To explore this possibility, we initially examined the effects of exogenous periostin on proliferation of normal human dermal fibroblasts (NHDFs). We confirmed that NHDFs proliferate in response to FGF2 (Fig. S6). We also found that proliferation of NHDFs was up-regulated in a dose-dependent manner of periostin coated on plates (Fig. 3a, $P < 0.05$ at periostin 0.1 μg/ml, 24 h, $P < 0.01$ at periostin 1 μg/ml, 24 h, $P < 0.001$ at periostin 0.1 or 1 μg/ml, 72 h and at periostin 0.1 or 1 μg/ml, 120 h). We then analysed the effects of periostin deficiency on proliferative activities of mouse dermal fibroblasts. Fibroblast cultures established from skin of newborn $Postn^{-/-}$ mice had impaired proliferation compared with fibroblasts from $Postn^{+/+}$ mice (Fig. 3b, $P < 0.05$ at 6 and 48 h, $P < 0.01$ at 24 h, $P < 0.001$ at 72 h). Treatment

with recombinant periostin slightly enhanced proliferation of fibroblasts from both wild-type (Fig. 3c, $P < 0.05$ at 72 h) and periostin-deficient ($P < 0.05$ at 12 and 24 h) mice. Further, we overexpressed retrovirally periostin in periostin-deficient fibroblasts and in wild-type fibroblasts (Fig. S7). As expected, these periostin-overexpressed cells had significantly up-regulated proliferation compared with mock-transfected wild-type (Fig. 3d, $P < 0.001$ at 24, 48, 60 and 72 h) or periostin-deficient (Fig. 3d, $P < 0.01$ at 60 and 72 h, $P < 0.001$ at 24 and 48 h) fibroblasts, respectively. These *in vitro* data demonstrate that either exogenously added or ectopically expressed periostin enhances the proliferative activities of fibroblasts.

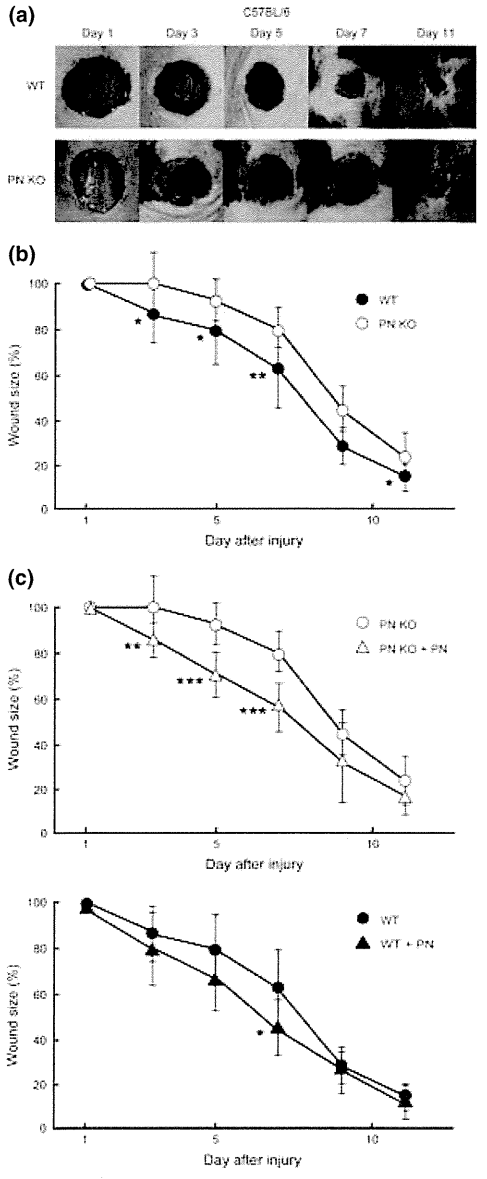

Figure 2. Periostin is important for efficient wound healing in mice. Successive photographs of the wounds (a), wound sizes at the indicated amount of days postinjury (b) in wild-type (WT, $n = 10$), or periostin-deficient mice (PN KO, $n = 10$) in C57BL/6 background. (c) Recombinant human periostin (+PN 2 μg) was injected intradermally into wounds of C57BL/6 background mice ($n = 10$ for each of WT and PN KO) every 2 days, from day 1 after injury to day 9. Wound sizes at the indicated times after injury (c). Statistical differences between PN KO vs WT, PN KO + PN vs PN KO and WT + PN vs WT are depicted. $*P < 0.05$, $**P < 0.01$, $***P < 0.001$.

Periostin enhances migration of dermal fibroblasts

We then examined the effects of periostin on migration of dermal fibroblasts using scratch wound cell monolayer method in wild-type and periostin-deficient MEFs (Fig. 4a,b). To exclude confounding effects upon proliferation, we arrested cell growth prior to analysis of migration. We confirmed that the migration activity of wild-type MEFs was up-regulated by platelet-derived growth factor (PDGF), whereas that was down-regulated by cytochalasin D (Fig. S8). The motility of periostin-deficient MEFs was significantly impaired compared with that of wild-type MEFs ($P < 0.05$ at 24 h). These results demonstrate that periostin can also enhance migration as well as the proliferation status of fibroblasts in response to wounding.

Discussion

It is well recognized that the ECM regulates the functions of the various cell lineages mobilized to the wounded area, contributing not only to re-epithelialization but also to granulation tissue formation and angiogenesis (35). Moreover, several studies using genetically deficient mice have shown that ECM proteins can play important *in vivo* functions during wounding and repair. For instance, fibronectin and its co-receptor, syndecan-4, are thought to accelerate wound repair as loss-of-function mouse mutants defective in the extra domain A of fibronectin or syndecan-4 both exhibit delayed cutaneous wound repair (36,37), whereas thrombospondin-1 and -2 play an opposite role and mainly inhibit wound repair (38,39). Based on previous observations that periostin is an ECM protein highly expressed during wound repair in various mouse models (32,33), in this study, we used periostin-deficient mice to test its requirement via our wound repair model. Meaningfully, both *in vivo* and *in vitro* results support the conclusion that periostin accelerates the wound healing process. Recently, using periostin-deficient mice, Nishiyama et al. (40) also reported that lack of periostin delays the process of cutaneous wound repair. Taking these results together, the requirement of periostin for the process of efficient cutaneous wound repair is well established.

The Nishiyama et al. (40) data indicated that periostin up-regulates keratinocyte proliferation and migration, accelerating the process of re-epithelialization. This result is consistent with our observation of significant periostin expression observed in the dermal–epidermal junction during wound repair. In our study, we similarly demonstrate that periostin enhances proliferation and migration of fibroblasts, which would contribute to the process of granulation tissue formation. We also demonstrated that periostin is deposited in fibroblast-enriched granulation tissues. Fibroblasts contribute to wound repair by generating several growth factors important for re-epithelialization (8) and by differentiating into α-SMA-expressing myofibroblasts important to close the wound edges by TGF-β1 (1–4). Collectively, these suggest that periostin deposition and the formation of fibroblast-enriched granulation tissues is the critical step during wound repair. The significance of fibroblast activation during wound repair is also supported by data from profibrotic cytokine, FGF2-null mice (41). Therefore, it is likely that direct or indirect activation of dermal fibroblasts by presence of periostin may be an additional mechanism underlying

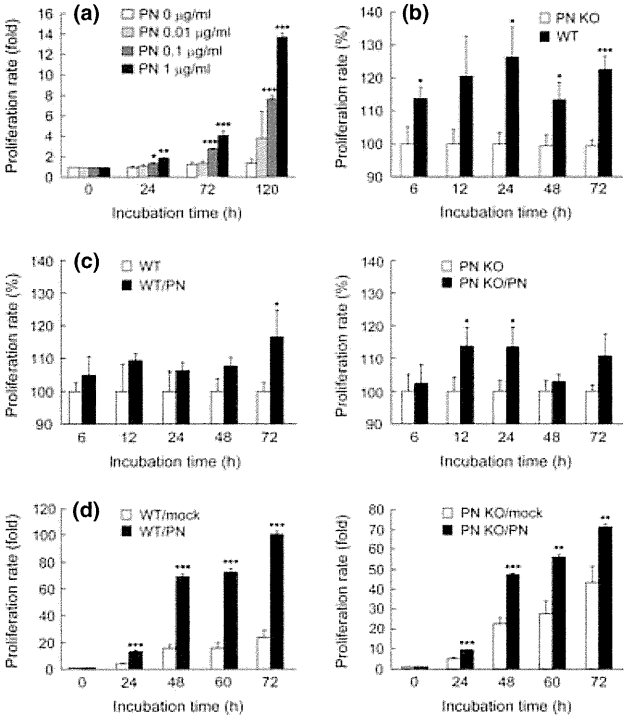

Figure 3. Effects of periostin on fibroblast proliferation. (a–c) Normal human dermal fibroblasts (a) or mouse dermal fibroblasts derived from wild-type (WT) or periostin-deficient mice (PN KO) (b, c) were cultured for various times. In panel (a), the concentrations of human periostin used are indicated, and in panel (c), 100 ng/ml of mouse periostin was used to coat the culture dishes. (d) Mouse periostin-overexpressed or mock-transduced MEFs (3×10^3 cells) derived from wild-type (WT) or periostin-deficient (PN KO) mice were cultured for various lengths. The proliferation rate was estimated using the Cell Counting Reagent SF. The relative folds were compared with the starting points (a, d) or PN KO-type or to fibroblasts on non-coated plates (b, c) are depicted. In panel (a), one-way ANOVA followed by Dunnett's test was used for multiple comparisons of the different fibroblast rates induced by various concentrations of periostin. Statistical differences were compared with PN 0 ng/ml cultures. Experiments were repeated five times, and the representative combined data are depicted. $^{*}P < 0.05$, $^{**}P < 0.01$, $^{***}P < 0.001$.

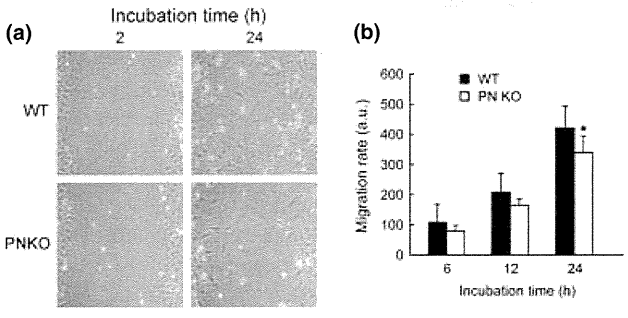

Figure 4. Effects of periostin on the migration of fibroblasts. Analysis of cell migration in MEFs derived from wild-type (WT) or periostin-deficient (PN KO) mice were compared. Photographs of the wounded cell monolayers at 2 and 24 h (a) and the relative cell motilities at various times indicated (b). The average cell motility (14 points per one field and three different fields/well in triplicate) was calculated and shown. Statistical difference between WT vs PN KO ($^{*}P < 0.05$) is depicted.

wound repair, in addition to periostin activation of keratinocytes (40).

It is well known that TGF-β1 is highly expressed in wounded tissues and can act as a central enhancer of wound repair effectors (42,43). Consequently, mice deficient in TGF-β1 show delayed cutaneous wound repair (44). When we examined whether TGF-β1 or other cytokines were able to directly induce periostin expression in human dermal fibroblasts and accumulated periostin in the supernatant was seen in responses to IL-4 and IL-13 (17,18) and to TGF-β1, whereas several other cytokines (IL-1β, -6, -17, tumor necrosis factor-α, FGF-2, FGF-5, stromal cell-derived factor-1, and PDGF) were not able to induce periostin expression (Fig. S9). Collectively, these results suggest that TGF-β1, abundant in the wound site, mainly contributes to periostin induction and that induction of periostin is a novel biological function of TGF-β1 within the well-ordered process of wound repair.

Targeted genetic deletion of periostin in mice significantly impairs fibroblast proliferation and wound healing, whereas fibroblast proliferation and wound healing can be enhanced by exogenous periostin, suggesting a direct role for periostin. Furthermore, treatment of dermal fibroblasts with exogenous periostin activates integrin-associated signalling molecules (FAK, STAT3, Akt and p44/42MAPK). As integrin-mediated signalling is initiated by formation of the Src/FAK complex, which enhances cell proliferation by up-regulating cyclin D1 expression via p44/42MAPK or cell survival by inhibiting proapoptotic factors such as Bad, caspase nine, forkhead transcription factors via PI3K/Akt (10–12), our results indicate that several levels of the proliferation pathway are activated when periostin is present. Moreover, STAT3 transduces signals important for cell proliferation and survival, cooperating with growth factor receptor-mediated signals (45,46). Periostin has been shown to induce proliferation of smooth muscle and/or cancer cells via the FAK/PI3K/Akt pathway (47,48). In contrast, genetic inhibition or administration of MAPK inhibitors delays wound repair (49,50). Finally, direct activation of the PI3K/Akt pathway is known to accelerate wound repair (51). These collective results suggest that periostin–integrins signal via FAK, STAT3, Akt and p44/42MAPK and play an important role in wound repair via augmenting cell proliferation/survival.

Clinically, it may be imperative to modulate either delayed (e.g. from diabetes or radiation exposure) or enhanced wound repair [e.g. hypertrophic and keloid scars (2,3)]. However, disappointing clinical results from single-agent therapies such as administering growth factors or other mediators to boost wound repair suggest that it is a highly ordered and complex process. Our surprising result, that injection of periostin into the wound in mice models can accelerate the healing process, may suggest that topical administration of periostin could be efficacious in wound treatment. Furthermore, it is now hoped that recent advances in stem cell/progenitor cell biology and material sciences will make it possible to entirely replace tissues. Our present data regarding the role of periostin in wound repair indicate that it could be a useful addition in construction of optimized skin tissues.

In conclusion, in this study, we demonstrate that periostin, transiently expressed during wound repair, accelerates the process by activating dermal fibroblasts. Although the pathological roles of periostin within fibrosis in various diseases have recently been well characterized, the physiological roles of periostin in skin repair are starting to be uncovered. Our present study demonstrates a novel physiological role for periostin: namely, its involvement in effective cutaneous wound repair.

Acknowledgements

We thank Dr. Dovie R. Wylie, Hiroyuki Ideguchi, Yumiko Ohishi, Yukako Kanazawa and Maiko Urase for critical review of this manuscript, technical and secretarial assistance. KO, YK, HS, SS and LY performed the research. AT, MF, YN, HM, ST, IK, KI and TN designed the research study. SO, KA, SS, AK and SJC contributed essential reagents or tools. KO, YK, SJC and KI wrote the paper. This work was supported in part by Grants-in-Aid for Scientific Research from the Japan Society for the Promotion of Science and by Grant-in-Aid from the Ministry of Health, Labour and Welfare, Japan.

Conflict of interests

The authors have no declared no conflicts of interests.

References

1 Baum C L, Arpey C J. Dermatol Surg 2005: **31**: 674–686.
2 Gurtner G C, Werner S, Barrandon Y *et al.* Nature 2008: **453**: 314–321.
3 Singer A J, Clark R A. N Engl J Med 1999: **341**: 738–746.
4 Palatinus J A, Rhett J M, Gourdie R G. J Mol Cell Cardiol 2010: **48**: 550–557.
5 Ranzato E, Martinotti S, Volante A *et al.* Exp Dermatol 2011: **20**: 308–313.
6 Kim J H, Jung M, Kim H S *et al.* Exp Dermatol 2011: **20**: 383–387.
7 Novotny M, Vasilenko T, Varinska L *et al.* Exp Dermatol 2011: **20**: 703–708.
8 Werner S, Grose R. Physiol Rev 2003: **83**: 835–870.
9 Desmouliere A, Geinoz A, Gabbiani F *et al.* J Cell Biol 1993: **122**: 103–111.
10 Eliceiri B P. Circ Res 2001: **89**: 1104–1110.
11 Giancotti F G, Ruoslahti E. Science 1999: **285**: 1028–1032.
12 Hynes R O. Trends Cell Biol 1999: **9**: M33–M37.
13 Hamilton D W. J Cell Commun Signal 2008: **2**: 9–17.
14 Rios H, Koushik S V, Wang H *et al.* Mol Cell Biol 2005: **25**: 11131–11144.
15 Midwood K, Sacre S, Piccinini A M *et al.* Nat Med 2009: **15**: 774–780.
16 Shinohara M L, Kim J H, Garcia V A *et al.* Immunity 2008: **29**: 68–78.
17 Hayashi N, Yoshimoto T, Izuhara K *et al.* Proc Natl Acad Sci U S A 2007: **104**: 14765–14770.
18 Takayama G, Arima K, Kanaji T *et al.* J Allergy Clin Immunol 2006: **118**: 98–104.
19 Woodruff P G, Boushey H A, Dolganov G M *et al.* Proc Natl Acad Sci U S A 2007: **104**: 15858–15863.
20 Okamoto M, Hoshino T, Kitasato Y *et al.* Eur Respir J 2011: **37**: 1119–1127.
21 Shimazaki M, Nakamura K, Kii I *et al.* J Exp Med 2008: **205**: 295–303.
22 Hakuno D, Kimura N, Yoshioka M *et al.* J Clin Invest 2010: **120**: 2292–2306.
23 Oku E, Kanaji T, Takata Y *et al.* Int J Hematol 2008: **88**: 57–63.
24 Yoshida S, Ishikawa K, Asato R *et al.* Invest Ophthalmol Vis Sci 2011: **52**: 5670–5678.
25 Blanchard C, Mingler M K, McBride M *et al.* Mucosal Immunol 2008: **1**: 289–296.
26 Sidhu S S, Yuan S, Innes A L *et al.* Proc Natl Acad Sci U S A 2010: **107**: 14170–14175.
27 Kuhn B, del Monte F, Hajjar R J *et al.* Nat Med 2007: **13**: 962–969.
28 Lorts A, Schwanekamp J A, Elrod J W *et al.* Circ Res 2009: **104**: e1–e7.
29 Fujimoto K, Kawaguchi T, Nakashima O *et al.* Oncol Rep 2011: **25**: 1211–1216.
30 Ruan K, Bao S, Ouyang G. Cell Mol Life Sci 2009: **66**: 2219–2230.
31 Snider P, Hinton R B, Moreno-Rodriguez R A *et al.* Circ Res 2008: **102**: 752–760.
32 Jackson-Boeters L, Wen W, Hamilton D W. J Cell Commun Signal 2009: **3**: 125–133.
33 Zhou H M, Wang J, Elliott C *et al.* J Cell Commun Signal 2010: **4**: 99–107.
34 Kitamura T, Koshino Y, Shibata F *et al.* Exp Hematol 2003: **31**: 1007–1014.
35 Midwood K S, Williams L V, Schwarzbauer J E. Int J Biochem Cell Biol 2004: **36**: 1031–1037.
36 Echtermeyer F, Streit M, Wilcox-Adelman S *et al.* J Clin Invest 2001: **107**: R9–R14.
37 Muro A F, Chauhan A K, Gajovic S *et al.* J Cell Biol 2003: **162**: 149–160.
38 Kyriakides T R, Tam J W, Bornstein P. J Invest Dermatol 1999: **113**: 782–787.
39 Streit M, Velasco P, Riccardi L *et al.* EMBO J 2000: **19**: 3272–3282.
40 Nishiyama T, Kii I, Kashima T G *et al.* PLoS One 2011: **6**: e18410.
41 Ortega S, Ittmann M, Tsang S H *et al.* Proc Natl Acad Sci U S A 1998: **95**: 5672–5677.
42 Barrientos S, Stojadinovic O, Golinko M S *et al.* Wound Repair Regen 2008: **16**: 585–601.
43 Werner S, Krieg T, Smola H. J Invest Dermatol 2007: **127**: 998–1008.
44 Crowe M J, Doetschman T, Greenhalgh D G. J Invest Dermatol 2000: **115**: 3–11.
45 Guo W, Pylayeva Y, Pepe A *et al.* Cell 2006: **126**: 489–502.
46 Shin H D, Park B L, Kim L H *et al.* Hum Mol Genet 2004: **13**: 397–403.
47 Bao S, Ouyang G, Bai X *et al.* Cancer Cell 2004: **5**: 329–339.
48 Li G, Jin R, Norris R A *et al.* Atherosclerosis 2010: **208**: 358–365.
49 Sharma G D, He J, Bazan H E. J Biol Chem 2003: **278**: 21989–21997.
50 Thuraisingam T, Xu Y Z, Eadie K *et al.* J Invest Dermatol 2010: **130**: 278–286.
51 Lai J P, Dalton J T, Knoell D L. Br J Pharmacol 2007: **152**: 1172–1184.

Supporting Information

Additional Supporting Information may be found in the online version of this article:

Figure S1. Periostin expression in wounded tissues.

Figure S2. Expression of periostin in the wound sites in mice.

Figure S3. Periostin is important for efficient wound healing in mice.

Figure S4. Periostin is important for efficient wound healing in mice.

Figure S5. Activation of human dermal fibroblasts by exogenous periostin.

Figure S6. Effects of fibroblast growth factor-2 on fibroblast proliferation.

Figure S7. Establishment of periostin-transduced MEFs.

Figure S8. Effects of cytochalasin D and platelet-derived growth factor on cell migration.

Figure S9. Analysis of periostin responses in human dermal fibroblasts to various stimuli.

Data S1. Materials and methods.

Please note: Wiley-Blackwell is not responsible for the content or functionality of any supporting materials supplied by the authors. Any queries (other than missing material) should be directed to the corresponding author for the article.

ORIGINAL ARTICLE

Serum Leucine-rich Alpha-2 Glycoprotein Is a Disease Activity Biomarker in Ulcerative Colitis

Satoshi Serada, PhD, Minoru Fujimoto, MD, PhD,* Fumitaka Terabe, MD, PhD,*† Hideki Iijima, MD, PhD,† Shinichiro Shinzaki, MD, PhD,† Shinya Matsuzaki, MD,‡ Tomoharu Ohkawara, MD,* Riichiro Nezu, MD, PhD,§ Sachiko Nakajima, MD, PhD,† Taku Kobayashi, MD, PhD,‖ Scott Eric Plevy, MD, PhD,‖ Tetsuo Takehara, MD, PhD,† and Tetsuji Naka, MD, PhD**

Background: Reliable biomarkers for monitoring disease activity have not been clinically established in ulcerative colitis (UC). This study aimed to investigate whether levels of serum leucine-rich alpha-2 glycoprotein (LRG), identified recently as a potential disease activity marker in Crohn's disease and rheumatoid arthritis, correlate with disease activity in UC.

Methods: Serum LRG concentrations were determined by enzyme-linked immunosorbent assay (ELISA) in patients with UC and healthy controls (HC) and were evaluated for correlation with disease activity. Expression of LRG in inflamed colonic tissues from patients with UC was analyzed by western blotting and immunohistochemistry. Interleukin (IL)-6-independent induction of LRG was investigated using IL-6-deficient mice by lipopolysaccharide (LPS)-mediated acute inflammation and dextran sodium sulfate (DSS)-induced colitis.

Results: Serum LRG concentrations were significantly elevated in active UC patients compared with patients in remission ($P < 0.0001$) and HC ($P < 0.0001$) and were correlated with disease activity in UC better than C-reactive protein (CRP). Expression of LRG was increased in inflamed colonic tissues in UC. Tumor necrosis factor alpha (TNF-α), IL-6, and IL-22, serum levels of which were elevated in patients with active UC, could induce LRG expression in COLO205 cells. Serum LRG levels were increased in IL-6-deficient mice with LPS-mediated acute inflammation and DSS-induced colitis.

Conclusions: Serum LRG concentrations correlate well with disease activity in UC. LRG induction is robust in inflamed colons and is likely to involve an IL-6-independent pathway. Serum LRG is thus a novel serum biomarker for monitoring disease activity in UC and is a promising surrogate for CRP.

(Inflamm Bowel Dis 2012;000:000–000)

Key Words: IBD, ulcerative colitis, biomarker, leucine-rich alpha-2 glycoprotein, DSS

The chronic inflammatory bowel diseases (IBDs), Crohn's disease (CD) and ulcerative colitis (UC), are typically characterized by episodes of acute flares and remission.[1,2] Depending on disease location and extent, exacerbation leads to diarrhea, abdominal pain, and systemic symptoms such as fatigue and weight loss.[3–5] Disease activity indices have been developed as outcome measures in clinical trials.[6,7] They may help to reproducibly and validly assess the patients' status and to support therapeutic decision-making.[6] Variables of disease activity indices comprise frequency of bowel movements, severity of abdominal pain, general well-being, occurrence of extra-intestinal manifestations, and laboratory parameters.[8]

One of the most important protein biomarkers increased during the inflammatory state is C-reactive protein (CRP). However, elevation of serum CRP levels is not observed in certain inflammatory diseases. While serum CRP levels are highly increased in CD and rheumatoid arthritis (RA) patients and widely used for monitoring

Additional Supporting Information may be found in the online version of this article.

Received for publication February 12, 2012; Accepted February 13, 2012.

From the *Laboratory for Immune Signal, National Institute of Biomedical Innovation, Osaka, Japan, †Department of Gastroenterology and Hepatology, Osaka University Graduate School of Medicine, Osaka, Japan, ‡Department of Obstetrics and Gynecology, Osaka University Graduate School of Medicine, Osaka, Japan, §Department of Surgery, Osaka Rosai Hospital, Osaka, Japan, ‖Center for Gastrointestinal Biology and Diseases, University of North Carolina School of Medicine, Chapel Hill, North Carolina, USA.

Supported by the Grant-in-Aid for Scientific Research (C) (22591101) from the Japanese Ministry of Education, Science, Sports, and Culture; a grant-in-aid for the Program for Promotion of Fundamental Studies in Health Sciences of the National Institute of Biomedical Innovation and Grant-in-Aid from the Ministry of Health, Labour and Welfare of Japan.

Reprints: Tetsuji Naka, Laboratory for Immune Signal, National Institute of Biomedical Innovation, 7-6-8, Saito-asagi, Ibaraki, Osaka 567-0085, Japan (e-mail: tnaka@nibio.go.jp).

DOI 10.1002/ibd.22936

Published online in Wiley Online Library (wileyonlinelibrary.com).

TABLE 1. Characteristics of Patients with Ulcerative Colitis (UC)

Characteristics	Patients with UC	Patients with Appendicitis and Diverticulitis
Number (male:female)	82 (41:41)	17 (8:9)
Age, yr, mean (SD)	40.1 (15.7)	33.1 (13.7)
Age at diagnosis, yr, mean (SD)	34.7 (15.6)	33.1 (13.7)
Bowel surgery (including appendectomy), *N* (%)	7 (8.54)	
Treatment		
Salazosulfapyridine or mesalazine, N (%)	66 (80.5)	
Steroids, *N* (%)	16 (19.5)	
Immunomodulators, *N* (%)	3 (3.7)	
Disease location (*N*)		
Extensive colitis/left-sided colitis/proctitis	37/30/15	
CRP, mg/dL, mean (SD)	0.884 (1.967)	8.47 (7.69)
WBC cells/μl, mean (SD)	6716 (2317)	12307 (3603)
CAI, mean (SD)	4.71 (4.89)	
Matts's score, mean (SD)	2.27 (0.89)	

disease activity, only modest to absent CRP responses are observed in systemic lupus erythematosus (SLE), dermatomyositis, Sjogren's syndrome, or UC, although active inflammation is present.[9–11] In UC, endoscopic disease activity may predict future clinical symptoms,[12] but direct endoscopic or radiologic visualization of the degree of inflammation is rarely performed in outpatients with inactive or mild disease. Therefore, alternative biomarkers, which can conveniently and precisely monitor disease activity during therapy in inflammatory diseases, are required for the determination of adequate treatment.

By using a quantitative proteomic approach, we have previously reported that serum levels of leucine-rich alpha-2 glycoprotein (LRG) were elevated in patients with active RA and serum LRG levels were correlated with disease activity of not only RA but also CD, suggesting that serum LRG is a serological biomarker for monitoring disease activity.[13] LRG is an ≈50 kDa glycoprotein and contains repetitive sequences with a leucine-rich motif, first purified from human serum.[14,15] LRG has been reported to be expressed by the liver cells and neutrophils[16,17]; however, its function remains unclear. To date, the relationship between serum LRG levels and disease activity in UC has not been assessed. In this study we investigated serum LRG expression levels in UC patients and evaluated their correlation with clinical disease activity. Serum LRG levels were significantly increased in the active UC patients. LRG expression was upregulated in the inflamed colonic mucosa of UC possibly through stimulation by various cytokines including tumor necrosis factor alpha (TNF-α), interleukin (IL)-6, and IL-22, the expression of which are increased in active UC. Moreover, we show that serum LRG correlates more strongly than CRP with disease activity in UC. Therefore, serum LRG may be a useful disease activity biomarker for UC.

MATERIALS AND METHODS

Patients and Sera

Sera were obtained from patients with UC ($n = 82$), appendicitis ($n = 13$), and diverticulitis ($n = 4$) and surgical or biopsy samples were obtained from patients with UC ($n = 10$) from Osaka University Hospital (Osaka, Japan) and the Department of Surgery, Osaka Rosai Hospital, respectively. Sera from healthy controls (HCs) ($n = 50$), age/sex-matched with UC patients, were used. Diagnosis of UC was based on conventional clinical, radiological, endoscopic, and histopathological criteria. Clinical activities were determined using the Clinical Activity Index (CAI) for UC.[18] Clinical remission was defined as CAI <6.[19] In addition to CAI, the endoscopic findings were also graded according to Matts' criteria.[20] Endoscopic remission was defined as Matts' score ≤ 2. Detailed patient characteristics are presented in Table 1. For Caucasian patients with UC, sera ($n = 30$) were obtained from the Department of Medicine, University of North Carolina Hospital (Chapel Hill, NC). Sera from HCs ($n = 19$), age/sex-matched with UC patients, were used. Detailed patient characteristics are presented in Table 2, while data of disease activity of UC is not available.

Quantification of Serum LRG and Cytokines

Human serum LRG and mouse serum LRG were quantitated by human LRG assay kit (IBL, Fujioka, Japan) and mouse LRG assay kit (IBL, Fujioka, Japan). These enzyme-linked immunosorbent assay (ELISA) assays were performed

TABLE 2. Characteristics of Patients with UC in a Caucasian Cohort

Characteristics	Patients with UC
Number (male:female)	30 (18:12)
Age, yr, mean (SD)	42.9 (17.9)
Age at diagnosis, yr, mean (SD)	33.2 (15.7)
Treatment	
Salazosulfapyridine or mesalazine, *N* (%)	14 (46.7)
Steroids, *N* (%)	9 (30.0)
Immunomodulators, *N* (%)	11 (36.7)
Anti-TNF therapy	3 (10.0)
Disease location (*N*)	
Extensive colitis/left-sided colitis/proctitis	16/11/3

in duplicate. The intraassay coefficients of variations for human LRG and mouse LRG were $\leq$7.98% and $\leq$8.93%, respectively. For the quantification of IL-6, TNF-α, and IL-22 in human serum samples, the human IL-6 Ultra Sensitive ELISA (Biosource International, Camarillo, CA), human TNF-α UltraSensitive ELISA kit (Invitrogen, Carlsbad, CA), and human IL-22 Quantikine ELISA Kit (R&D Systems, Minneapolis, MN) were used following the manufacturer's guidelines.

Western Blot Analysis

Frozen colon tissue samples were lysed in RIPA buffer (10 mM Tris-HCl, pH 7.5, 150 mM NaCl, 1% Nonidet P-40, 0.1% sodium deoxycholate, 0.1% SDS, 1 × protease inhibitor cocktail; Nacalai Tesque, Kyoto, Japan) and 1 × phosphatase inhibitor cocktail (Nacalai Tesque) followed by centrifugation (13,200 rpm, 4°C, 15 minutes), after which the supernatants were stored at −80°C until use. Extracted proteins were subjected to sodium dodecyl sulfate-polyacrylamide gel electrophoresis (SDS-PAGE) as described previously.[21] Samples transferred onto PVDF membranes were treated with a rabbit antihuman LRG polyclonal antibody (Proteintech Group, Chicago, IL) or a rabbit anti-GAPDH polyclonal antibody (Santa Cruz Biotechnology, Santa Cruz, CA) was used as described previously.[21]

Immunohistochemistry

Immunohistochemical analyses were performed according to a method described in our previous report.[22] Briefly, rabbit antihuman LRG polyclonal antibodies were used as the primary antibody. After incubation with the primary antibodies, the sections were treated with biotin-conjugated goat anti-rabbit IgG (Vector Laboratories, Burlingame, CA) and avidin-biotin-peroxidase complexes (Vector Laboratories). Immunoreactive cells were visualized with a diaminobenzidine substrate (Merck, Darmstadt, Germany) and were counterstained with hematoxylin.

Mice

C57BL/6 mice were purchased from Clea Japan (Tokyo, Japan). C57BL/6-background IL-6-deficient mice were kindly provided by Professor Yoichiro Iwakura (Laboratory of Molecular Pathogenesis, Center for Experimental Medicine, Institute of Medical Science, University of Tokyo, Tokyo, Japan). Mice were maintained under specific pathogen-free conditions. C57BL/6 and IL-6-deficient mice were used at 7–9 weeks of age. All experiments were conducted according to the institutional ethical guidelines for animal experimentation.

LPS-mediated Acute Inflammation

To induce acute inflammation, wildtype (WT) mice and IL-6-deficient mice were injected intraperitoneally with 0 or 10 mg/kg LPS (*Escherichia coli* LPS, Sigma, St. Louis, MO) dissolved in 500 μL phosphate-buffered saline (PBS). Blood was collected at before and 24 hours after LPS injection and the serum was separated by centrifugation and stored at −30°C until used for ELISA analysis.

Induction of Colitis

For induction of colitis, WT mice and IL-6-deficient mice were given 3% dextran sodium sulfate (DSS) (m/w 36,000–50,000; MP Biomedicals, Solon, OH) dissolved in drinking water provided ad libitum for 5 days, followed by provision of ordinary water for 20 days.

Assessment of Severity of DSS-induced Colitis

WT mice were weighed daily from day 0 to day 25. Changes in body weight were calculated as follows: body weight change (%) = [(weight on a given day (days 0–13) − weight on day 0)/weight on day 0] * 100. Blood was collected from WT mice on days 5, 7, 10, 15, and 25 after DSS administration or day 0 by cardiac puncture under anesthesia and on days 0 and 10 from IL-6-deficient mice. The serum was separated by centrifugation and stored at −30°C until used for ELISA analysis.

Cell Culture

The human colonic adenocarcinoma COLO205 cell line was obtained from the American Type Culture Collection (ATCC, Manassas, VA). Cells were maintained in RPMI 1640 medium supplemented with 10% fetal bovine serum (FBS) (HyClone Laboratories, Logan, UT) and 1% penicillin–streptomycin (Nacalai Tesque) at 37°C under a humidified atmosphere of 5% CO_2.

For the analysis of LRG protein induction, COLO205 cells were stimulated with various concentrations of cytokines for 24 hours and culture supernatant were concentrated using Amicon Ultra-4 10K MWCO (Millipore, Bedford, MA). Concentrated supernatants were used for western blot analysis. Full-length human LRG cDNA was inserted into pcDNA3.1/V5-His-TOPO vector (Invitrogen) and designated pcDNA3.1-LRG-V5-His. pcDNA3.1-LRG-V5-His vector was transfected

into COS7 cells using Lipofectamine 2000 reagent (Invitrogen) and culture medium were used for the positive control.

Quantitative Real-time Reverse-transcription Polymerase Chain Reaction (RT-PCR) Analysis

For the quantification of mRNA levels of LRG, various mouse organs were analyzed by real-time RT-PCR as described previously.[23] Levels of mouse LRG and mouse hypoxanthine phosphoribosyltransferase (HPRT) levels were determined by the 7900HT Real-time PCR system (Applied Biosystems, Foster City, CA) using specific primers: murine LRG forward 5′-ATCAAGGAAGCCTCCAGGAT-3′; reverse 5′-CAGCTGCGTCAGGTTGG-3′ and murine hypoxanitine phosphoribosyltransferase (HPRT) forward 5′-TCAGTCAACG GGGGACATAAA-3′; reverse 5′-GGGGCTGTACTGCTT AACCAG-3′.

Statistics

The Mann–Whitney *U*-test or one-way analysis of variance (ANOVA) followed by a Scheffe's test were used for statistical analyses. Two-tailed Student's *t*-test was used for significant differences in LRG expression between identical patients with UC in active and remission disease stage. One-way ANOVA followed by a Dunnett's test was used for multiple comparison of the difference of serum LRG levels at various timepoints after DSS treatment in mice. Pearson's test was used to analyze the relationship between LRG and CRP, IL-6, or CAI. For drawing of receiver operating characteristic (ROC) curves and estimation of the area under the ROC curve (AUC) statistics, the software Excel Statistics 2010 (Social Survey Research Information, Tokyo, Japan) was used to quantify the ability to differentiate between remission and active by CAI. $P < 0.05$ was considered significant.

Ethical Considerations

Informed consent was obtained from all donors and all studies involving human subjects were approved by the Institutional Review Boards of the National Institute of Biomedical Innovation, Osaka University Hospital, the Department of Surgery, Osaka Rosai Hospital, and the University of North Carolina.

RESULTS

Serum LRG Levels Are Increased in Active UC Patients

We quantified serum LRG concentrations by ELISA using sera from patients with UC. Serum LRG concentrations were significantly elevated in the active UC patients (CAI ≥6) (14.24 ± 8.08 μg/mL) compared with HC (3.07 ± 1.42 μg/mL; $P < 0.0001$) (Fig. 1A). There was also a significant difference between LRG serum levels in patients with active UC (CAI ≥6) (14.24 ± 8.08 μg/mL) compared with UC in remission (CAI <6) (5.34 ± 2.60 μg/mL; $P <$ 0.0001) (Fig. 1A). To determine whether serum LRG levels are increased in non-IBD disease controls, we quantified serum LRG levels in patients with appendicitis and

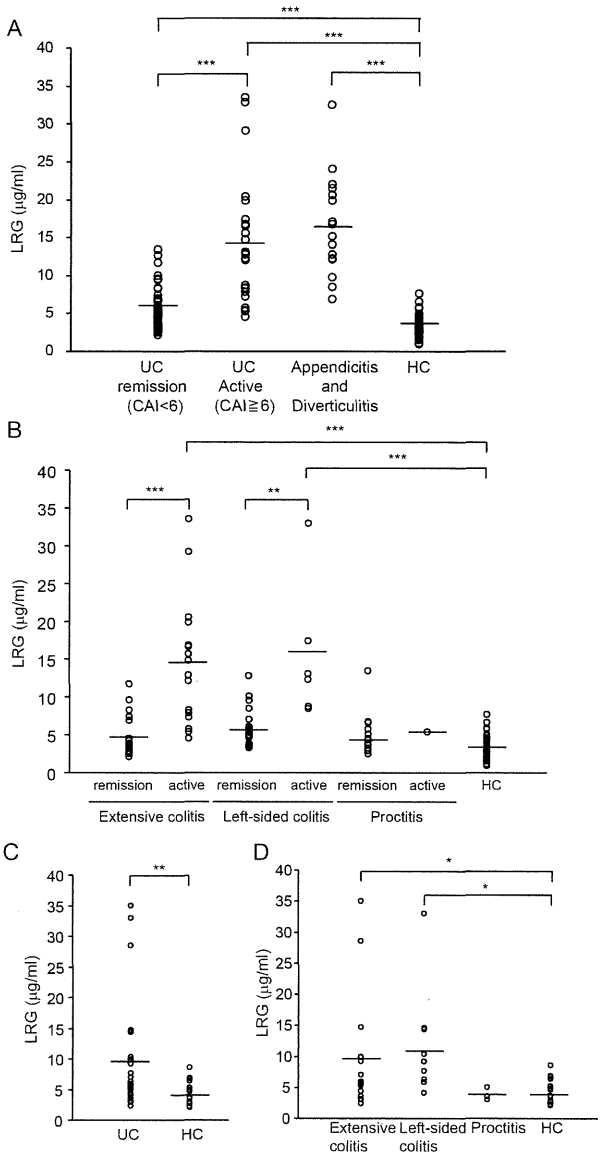

FIGURE 1. Serum LRG levels are increased in patients with active UC. (A) Serum levels of LRG were determined in 82 patients with UC (57 patients in remission [CAI <6], 25 patients in active [CAI ≥6] stage), appendicitis ($n = 13$), diverticulitis ($n = 4$) and 50 healthy controls (HC). ***$P < 0.0001$ by one-way ANOVA followed by Scheffe's post-hoc test. (B) Disease extension in UC was grouped into three categories: In UC patients in remission, extensive colitis ($n = 19$), left-sided colitis ($n = 24$), and proctitis ($n = 14$); in active patients, extensive colitis ($n = 18$), left-sided colitis ($n = 6$), and proctitis ($n = 1$) and HC ($n = 50$). **$P < 0.005$, ***$P < 0.0001$ by one-way ANOVA followed by Scheffe's post-hoc test. (C) Serum levels of LRG were determined in patients with UC ($n = 30$) and HC ($n = 19$) in a Caucasian cohort. **$P < 0.005$ by Mann–Whitney *U*-test. (D) In a Caucasian cohort, disease extension in UC was grouped into three categories: extensive colitis ($n = 16$), left-sided colitis ($n = 11$), and proctitis ($n = 3$) and HC ($n = 19$). *$P < 0.05$ by one-way ANOVA followed by Scheffe's post-hoc test.

diverticulitis. Elevated serum LRG levels were also observed in appendicitis and diverticulitis (16.83 ± 6.50 μg/mL) compared with HC (3.07 ± 1.42 μg/mL; $P < 0.0001$) (Fig. 1A), suggesting that serum LRG levels are also increased in acute intestinal inflammation.

When UC were classified into three categories based on disease extent, significantly higher serum LRG concentrations were observed in active patients with extensive colitis (14.34 ± 7.89 μg/mL) compared with in remission (4.96 ± 2.68 μg/mL; $P < 0.0001$) and HC (3.07 ±1.42 μg/mL; $P < 0.0001$) and active patients with left-sided colitis (15.41 ± 9.16 μg/mL) compared with in remission (5.91 ± 2.41 μg/mL; $P = 0.0003$) and HC (3.07 ±1.42 μg/mL; $P = 0.001$) (Fig. 1B). Nonetheless, there was no clear difference between active patients with proctitis and HC, possibly due to the low number of patients in this group. In patients with UC in remission, serum LRG levels in all of three disease extent categories were comparable with HC (Fig. 1B). Significantly elevated serum LRG levels were also detected in a Caucasian UC cohort (9.46 ± 8.44 μg/mL) compared with HC (4.42 ± 1.91 μg/mL; $P < 0.005$) (Fig. 1C). In this Caucasian UC cohort, serum LRG levels were also significantly elevated in patients with extensive colitis (9.54 ± 8.05 μg/mL) compared with HC (4.42 ± 1.91 μg/mL; $P < 0.05$) and left-sided colitis (10.90 ± 9.16 μg/mL) compared with HC (4.42 ± 1.91 μg/mL; $P < 0.02$) (Fig. 1D). However, a clear difference was not observed between patients with proctitis and HC (Fig. 1D). These results suggest that serum LRG levels were elevated in active UC.

Serum LRG Levels Are Correlated with Disease Activity in UC Patients

We investigated the correlation between serum LRG levels and disease activity (CAI) in UC patients. A positive correlation was observed between LRG and CAI ($r = 0.731$, $P < 0.00001$) (Fig. 2A). This correlation was stronger than that observed between CRP and CAI ($r = 0.654$, $P < 0.00001$) (Fig. 2A). When patients with UC were classified into active and remission according to the endoscopic findings, significantly elevated serum LRG levels and CRP levels were observed in patients with active UC compared with patients in remission ($P < 0.005$, respectively) (Supporting Fig. 1A). While serum LRG levels were significantly correlated with CRP levels in patients with UC ($r = 0.850$, $P < 0.00001$, $n = 82$) (Supporting Fig. 2A), such a correlation was not found when a CRP-negative subgroup (CRP <0.2, $n = 51$) was analyzed ($r = 0.101$, $P = 0.481$) (Supporting Fig. 2B). In this CRP-negative group, serum LRG levels were significantly correlated with CAI ($r = 0.416$, $P = 0.00241$) (Supporting Fig. 2C); however, significant correlation was not found between CRP and CAI ($r = -0.0896$, $P = 0.532$) (Supporting Fig. 2D). Additionally, in the CRP-negative group elevated serum LRG levels were detected in patients with endoscopically active UC compared with patients with UC in remission ($P = 0.0442$) (Supporting Fig. 1B). These findings in patients with low CRP may explain a better correlation of CAI with LRG than that with CRP.

When UC was classified by disease extent, a significantly higher positive correlation was detected between LRG and CAI than CRP and CAI both in extensive colitis ($r = 0.690$, $P < 0.000001$ and $r = 0.580$, $P = 0.000168$) and left-sided colitis ($r = 0.840$, $P < 0.000001$ and $r = 0.759$, $P < 0.000001$), but not in proctitis (Fig. 2B). Importantly, by analyzing sera obtained at active (CAI ≥6) and remission (CAI <6) disease stages from 10 identical UC patients, a significant decrease in serum LRG levels in remission was detected (Fig. 2C).

By generating an ROC curve, the sensitivity and specificity of serum LRG for remission and active by CAI were determined (Fig. 2D). The AUC for serum LRG levels was 0.901, whereas the AUC for CRP levels was 0.845. The cutoff value of serum LRG levels was 7.21 μg/mL (sensitivity = 84.0%, specificity = 82.5%). In contrast, when the cutoff value of CRP levels was set to 0.20, a maximum CRP value of normal range, the sensitivity was 80.0% and the specificity was 80.7%. These results emphasize the usefulness of monitoring serum LRG levels for the evaluation of the disease activity of UC.

Expression of LRG Was Increased in Inflamed UC Colons

Next, to investigate whether local inflammatory sites in patients with UC are a potential source of increased serum LRG we first looked at the expression of LRG in the colon by western blot analysis on inflamed and noninflamed sites of surgically resected full-thickness colon specimens from patients with UC. Western blot analysis showed that LRG expression in colon tissues was increased in inflamed sites of active UC patients compared with noninflamed colon tissues (Fig. 3A). Next, we tried to examine the localization of LRG. By immunohistochemistry, increased expression of LRG was detected in the cytoplasm of intestinal epithelial cells (IECs) in inflamed tissues (Fig. 3B–E). In contrast, expression of LRG was lower in noninflamed tissues (Fig. 3B–E). These data suggest that inflamed colon tissue is a potential source of increased serum LRG in patients with UC.

LRG Is Induced by Stimulation with TNF-α, IL-6, or IL-22

It has been reported that IL-6 is an inducer of LRG expression.[16] However, it is not clear whether LRG is induced by cytokines other than IL-6. At first we investigated the serum levels of IL-6, IL-22, and TNF-α, known

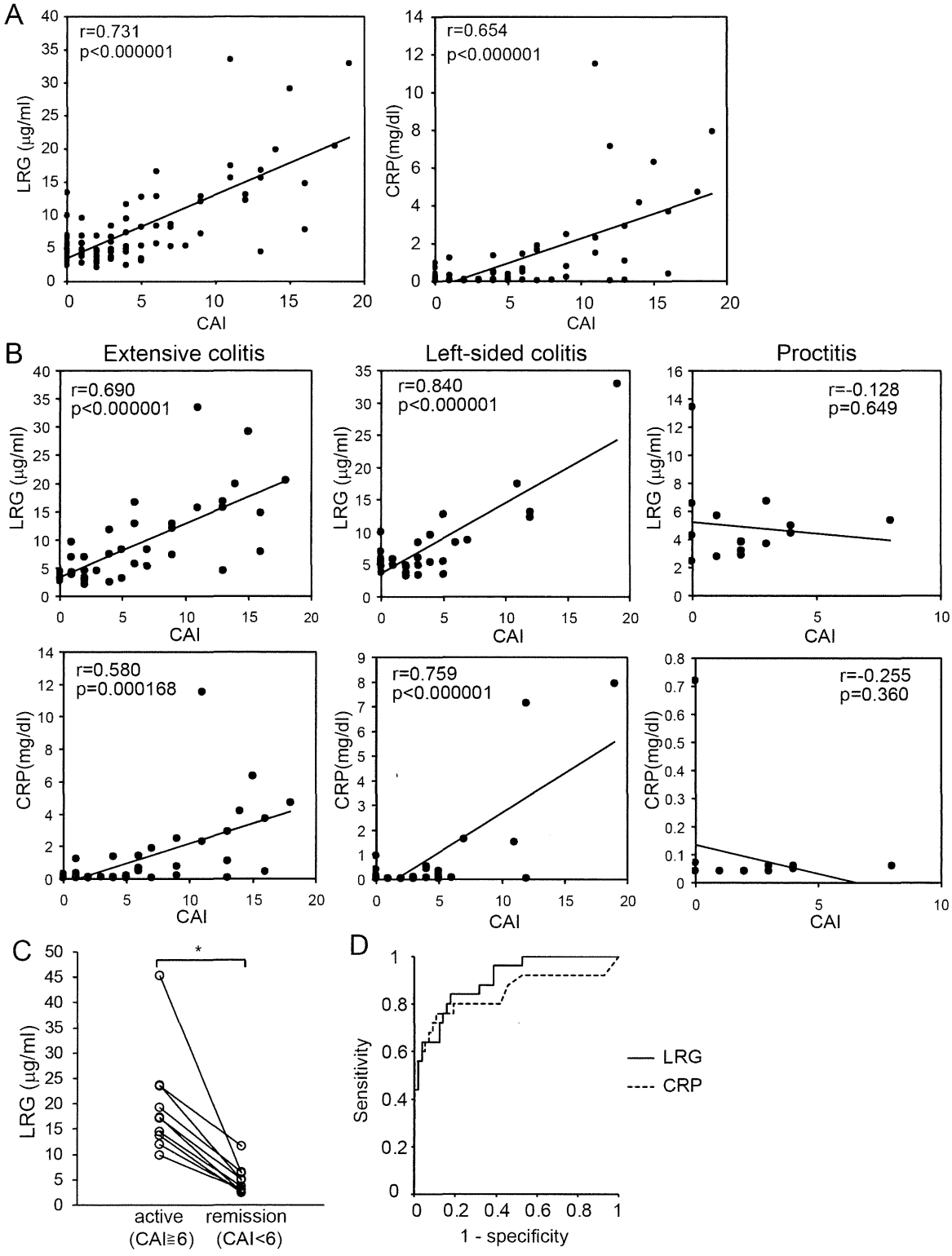

FIGURE 2. Serum LRG levels are correlated with disease activity better than CRP in patients with UC. (A) Serum levels of LRG correlated with CAI ($n = 82$; $P < 0.000001$; $r = 0.731$) better than CRP ($n = 82$; $P < 0.000001$; $r = 0.654$) in patients with UC. (B) Serum levels of LRG correlated with disease activity in extensive colitis ($n = 37$; $P < 0.000001$; $r = 0.690$) and left-sided colitis ($n = 30$; $P < 0.000001$; $r = 0.840$) better than CRP in extensive colitis ($n = 37$; $P = 0.000168$; $r = 0.580$) and left-sided colitis ($n = 30$; $P < 0.000001$; $r = 0.759$), while neither LRG ($n = 15$; $P = 0.649$; $r = -0.128$) nor CRP levels ($n = 15$; $P = 0.360$; $r = -0.255$) were correlated with disease activity in proctitis. (C) Compared with 10 identical active patients with UC, serum levels of LRG were decreased in remission. *$P < 0.002$ by Student's t-test. (D) ROC curves for LRG and CRP for differentiation between UC patients with remission ($n = 57$) and active ($n = 25$) by CAI.

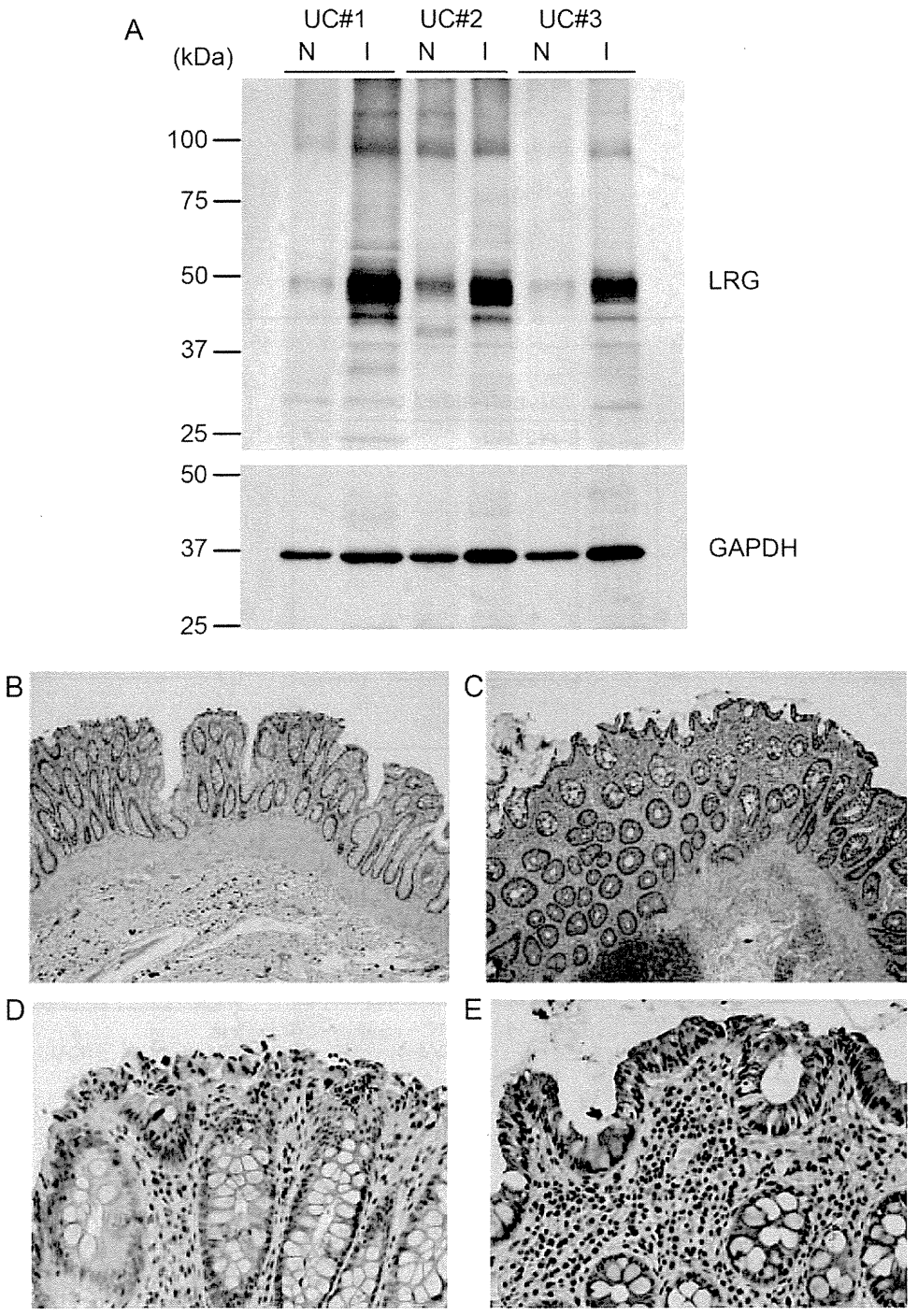

FIGURE 3. Expression of LRG is increased in lesion sites of ulcerative colitis. (A) Representative western blot analysis of three separate experiments for LRG using paired surgically resected full-thickness colon specimens from noninflamed (N) and inflamed (I) sites in patients with UC. GAPDH was used as a control of the relative amounts of proteins in each sample. Full-thickness colon tissues from UC in inflamed and noninflamed sites were evaluated by immunohistochemical analysis for LRG expression (n = 10 per experimental group). (B) Noninflamed mucosa (×42). (C) Inflamed mucosa from active UC (×42). (D) Noninflamed mucosa (×400). (E) Inflamed mucosa from active UC (×400).

to be increased at the inflamed tissue in active UC.[24–26] Indeed, ELISA analysis using sera from 82 UC patients revealed that serum TNF-α, IL-6, and IL-22 levels were significantly elevated in active UC patients compared with those patients in remission (P = 0.0178, P = 0.00690, and P < 0.0001, respectively) (Fig. 4A). Next, to investigate

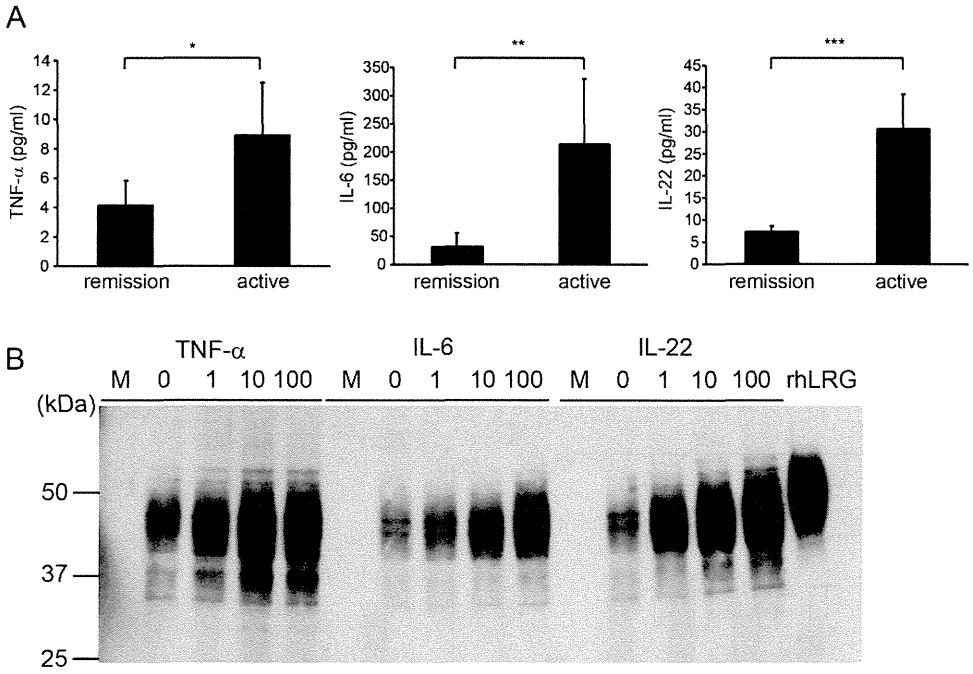

FIGURE 4. Expression of LRG was induced by TNF-α, IL-6, and IL-22. (A) Serum levels of TNF-α, IL-6, and IL-22 were determined in patients with UC (57 patients in remission [CAI <6] and 25 patients in active [CAI ≥6] stage). Data are expressed as mean ± SEM. *$P < 0.05$, **$P < 0.005$, ***$P < 0.0001$ by Mann–Whitney U-test. (B) LRG was determined in supernatants of COLO205 cells left untreated or stimulated with TNF-α, IL-6, and IL-22 at 1.0, 10, 100 ng/mL for 24 hours and analyzed by western blotting. There was a dose-dependent increase in LRG levels after treatment with TNF-α, IL-6, and IL-22.

which proinflammatory cytokines induce expression of LRG we stimulated human colonic adenocarcinoma COLO205 cells with TNF-α, IL-6, or IL-22 for 24 hours. After cytokine stimulation, secretion of LRG protein into the culture media was analyzed by western blotting. Interestingly, LRG was induced not only by stimulation with IL-6, but also by TNF-α and IL-22 in a dose-dependent manner (Fig. 4B). These results indicate that expression of LRG is induced by various proinflammatory cytokines including IL-6.

Expression of LRG Through an IL-6-independent Pathway Is Demonstrated in LPS-mediated Acute Inflammation and DSS-induced Colitis

CRP is one of the representative acute phase proteins in humans and CRP production is primarily dependent on liver by circulating IL-6. To examine the possible differences in induction mechanisms between LRG and CRP, particularly with regard to the involvement of IL-6, we took advantage of murine models. We first assessed whether LRG is induced in WT mice by injecting LPS, an inducer of proinflammatory cytokines from macrophages, because CRP is poorly induced in mice during acute inflammation. At 24 hours after intraperitoneal injection of LPS, serum samples were prepared and serum LRG levels were determined by ELISA. Compared with WT mice, significant elevation of serum LRG levels were detected in LPS-administered WT mice (Fig. 5A), suggesting that LRG is induced during acute inflammation in mice as in humans.

We next used a murine IBD model to investigate induction mechanisms of LRG during colonic inflammation. DSS-induced colitis is often used as a murine model of UC.[27] We induced colitis in WT mice by treating them with 3% DSS for 5 days and measured changes in relative body weight. Body weight began to decrease at day 5, showed greatest reduction at day 9, and recovered at 18 days after DSS treatment (Fig. 5B). We analyzed changes in serum LRG levels by ELISA before and 5, 7, 10, 15, and 25 days after DSS treatment. Consistent with body weight loss, serum LRG levels were significantly elevated at 5 days after DSS treatment (Fig. 5C). Serum LRG levels remained high until day 15, but decreased at day 25. Delayed normalization of serum LRG levels is likely due to the prolonged inflammation at inflamed tissue sites. Additionally, a long half-life of serum LRG might also be involved in this, since our preliminary data suggest that the half-life of serum human LRG levels are about two times longer than that of CRP (data not shown). To investigate which organs produce LRG in DSS-induced colitis, RNA was extracted from colon, liver, and spleen before and 9 days after DSS treatment. By quantitative PCR analysis (Fig. 5D), expression of LRG was significantly increased in liver ($P = 0.00106$) and spleen ($P = 0.0376$);